

Robust Hybrid Global Dual Quaternion Pose Control of Spacecraft-Mounted Robotic Systems

Matthew King-Smith* and Panagiotis Tsiotras Georgia Institute of Technology, Atlanta, Georgia 30332

https://doi.org/10.2514/1.G007598

We propose a nonlinear hybrid dual quaternion feedback control law for multibody spacecraft-mounted robotic systems (SMRSs) pose control. Indeed, screw theory expressed via a unit dual quaternion representation and its associated algebra can be used to compactly formulate both the forward (position and velocity) kinematics and pose control of N-degree-of-freedom robot manipulators. Recent works have also established the necessary theory for expressing the rigid multibody dynamics of an SMRS in dual quaternion algebra. Given the established framework for expressing both kinematics and dynamics of general N-body SMRSs via dual quaternions, this paper proposes a dual quaternion control law that achieves simultaneous global asymptotically stable pose tracking for the end effector and the spacecraft base of an SMRS. The proposed hybrid control law is robust to chattering caused by noisy feedback and avoids the unwinding phenomenon innate to continuous-based (dual) quaternion controllers. Additionally, an actuator allocation technique is proposed in the neighborhood of system singularities to ensure bounded control inputs, with minimum deviation from the specified spacecraft base and end-effector trajectories during controller execution.

Nomenclature						
$blkdiag(\cdot)$	=	creates a matrix whose diagonal contains				
		blocks of smaller matrices				
C_{ij}	=	connectivity adjacency matrix of the bodies				
		and joints				
H	=	set of quaternions				
\mathbb{H}_d	=	set of dual quaternions				
\mathbb{H}^r_d	=	set of dual scalar quaternions with zero dual				
\mathbb{H}^u	_	part set of unit quaternions				
	=	set of unit quaternions set of unit dual quaternions				
\mathbb{H}^u_d \mathbb{H}^v	=	set of unit dual quaternions set of vector quaternions				
\mathbb{H}_d^v	_	set of dual vector quaternions				
	=	controller gain matrices				
$ar{\ell}^{K_{\mathcal{B}_1},\ K_{\mathcal{G}}}$	=	error incurred in tracking				
M_{R}		dual inertia matrix of body B				
	=	controller scalar gains				
$p_{\mathcal{B}_1}, p_{\mathcal{G}}, k_{\mathcal{B}_1}, k_{\mathcal{G}}$ $Q_{\mathrm{L}}(\cdot), Q_{\mathrm{R}}(\cdot)$	=	C				
$\mathcal{Q}_{L}(\cdot), \mathcal{Q}_{R}(\cdot)$	_	shorthand for left and right dual quaternion multiplication, respectively				
ania	=	unit quaternion that represent orientation of				
$q_{\mathcal{B}/\mathcal{I}}$		frame \mathcal{B} with respect to frame \mathcal{I}				
$oldsymbol{q}_{\mathcal{B}/\mathcal{I}}$	=	unit dual quaternion that represent pose of				
1 5/1		frame \mathcal{B} with respect to frame \mathcal{I}				
$\mathbb{R}^{m \times n}$	=	set of $m \times n$ -dimensional real-valued matrices				
\mathbb{R}^n	=	set of <i>n</i> -dimensional real-valued column				
		vectors				
$\mathtt{S}(\cdot)$	=	swap components of a matrix				
$s(\cdot)$ $r_{\mathrm{B/O}}^{\mathcal{B}}$ $\bar{r}_{\mathrm{B/O}}^{\mathcal{B}}$	=	position quaternion given as $(0, \bar{r}_{B/O}^{B})$				
$\bar{r}_{R/G}^{\mathcal{B}}$	=	position vector of point B with respect to				
, B/O		point O as expressed in frame \mathcal{B}				
S ₁₁	=	blkdiag $(M_{\rm B_1} \cdots M_{\rm B_i} \cdots M_{\rm B_N})$				
S_{12}, S_{21}	=	matrices of coordinate transformations				
T	=	collection of all dual reaction wrenches				
u	=	collection of dual actuation wrenches				

Received 12 March 2023; revision received 29 July 2023; accepted for publication 27 August 2023; published online 17 October 2023. Copyright © 2023 by the American Institute of Aeronautics and Astronautics, Inc. All rights reserved. All requests for copying and permission to reprint should be submitted to CCC at www.copyright.com; employ the eISSN 1533-3884 to initiate your request. See also AIAA Rights and Permissions www.aiaa.org/randp.

[†]David & Andrew Lewis Chair and Professor, School of Aerospace Engineering; tsiotras@gatech.edu. Fellow AIAA.

\bar{u}	=	output singular vector
$\text{vec}(\cdot)$	=	set scalar component of (real and dual) qua-
		ternion to zero
$W^{\mathcal{B}}_{B}(O_{\mathcal{B}})$	=	dual wrench applied to body B at point O_B as
B		expressed in frame \mathcal{B}
\bar{x}	=	spacecraft-mounted robotic system state
		vector
0	=	$(0,0_{3\times 1})$
0	=	
$ \begin{array}{l} 0 \\ \overline{0}_{3\times 1} \end{array} $		$[0, 0, 0]^{T}$
1	=	$(1,\bar{0}_{3\times 1})$
1	=	$1+\epsilon 0$
α	=	scalar dynamic memory state function
Г, Г, Г	=	collection of generalized joint coordinates,
		rates, and accelerations of manipulators
γ	=	maximum permissible norm control value
$rac{\Delta}{\delta}$	=	size of singular region
	=	hysteresis half-width
ϵ	=	dual unit
η	=	right-hand side of the proposed control law
κ	=	matrix condition number
$\lambda,eta \ ar{\mu}$	=	allocation dampening factors
μ	=	collection of reduced real-valued actuation
-B		wrenches
$ar{v}_{\mathrm{B/O}}^{\mathcal{B}}$	=	linear velocity vector of point B with respect
Ξ	_	to point O as expressed in frame B
Π_i	=	blkdiag $(\Pi_{B_1}, \Pi_1, \dots, \Pi_j, \dots, \Pi_{N-1})$
\mathbf{n}_{j}	=	projection matrix mapping dual velocity joint rates to generalized joint rates
σ	=	matrix singular value
<i>0</i> v	=	collection of all dual body velocities
$\Phi(\bar{x}), \Psi(\bar{x})$	=	dynamics vector and matrices of spacecraft-
$\Psi(\lambda), \Gamma(\lambda)$	_	dynamics vector and matrices or spacecraft-

mounted robotic systems, respectively dual velocity of body B with respect to frame \mathcal{I} angular velocity vector of frame \mathcal{B} with respect to frame \mathcal{I} as expressed in frame \mathcal{B}

velocities to generalized rates

dual quaternion circle product

(dual) quaternion conjugation

ternion

8-by-8 matrix

projection operators mapping joint dual

denotes a real-valued column vector or

removes the zeros from a vector dual qua-

multiplication of dual quaternions with an

5

 $[*]Robotics\ Ph.D.\ Candidate,\ School\ of\ Electrical\ and\ Computer\ Engineering;\ mcks \\ 3@gatech.edu.$

 $[\cdot]$

(·)s = swap the dual and real quaternions components of dual quaternions
 (·,·) = shorthand for ordered pair representing a quaternion, i.e., ℝ × ℝ³ → ℍ

= bijective mapping between the set of dual

quaternions and \mathbb{R}^8 $[\cdot]^{\times}$ = skew-symmetric matrix operator

 $[\cdot]_L, [\cdot]_R$ = left and right quaternion multiplication,

 $[\![\cdot]\!]_L, [\![\cdot]\!]_R$ = left and right dual quaternion multiplication, respectively

Subscripts and superscripts

 B_i, J_j = *i*th body and *j*th joint

 $\mathcal{B}_i, \mathcal{J}_j, \mathcal{G}$ = *i*th body, *j*th joint, and end-effector frames

 \mathcal{E}, \mathcal{S} = reference frames

I. Introduction

N-SPACE assembly and manufacturing (ISAM) holds the promise to refuel, maintain, upgrade, and repair existing spacecraft; enable space construction; and actively remove orbital debris [1–3]. During an ISAM mission, involving close-proximity operations with other space objects, the servicing spacecraft must adapt to a changing environment and simultaneously achieve the primary mission objective(s). Although some ISAM missions may only need spacecraft-mounted robotic systems (SMRSs) to stabilize the relative kinematics between the servicer spacecraft and the target satellite, future missions may require multi-objective, multibody maneuvering such as requiring a single point of contact between two satellites at the end effector, while also controlling the spacecraft base to maintain line of sight with Earth for communication purposes. In such cases, simultaneous precise end-effector control of the maneuvering satellite and the spacecraft base is required.

Unlike the traditional, fully decoupled, 6-degree-of-freedom (6-DOF) relative pose control problem of spacecraft [4], SMRSs have manipulators that add an additional *N*-DOF to the system. This (6+N)-DOF control problem is challenging to solve using existing conventional control methods [5]. Typical approaches to solve this multi-DOF SMRS control problem are roughly divided into two categories: internal control and coordinated control. The first approach disables the attitude control system of the spacecraft base, leaving the SMRS in a free-floating state [6]. Thus, end-effector control must be planned such that the system's manipulator(s) achieves control objective(s) while also compensating for the reactive motion of the spacecraft base.

Although the internal control approach saves fuel during a maneuver, the approach requires significantly more complicated control strategies and is highly dependent on the SMRS topology [7]. Additionally, due to the nonstationary base, the velocity of the end effector is affected not only by kinematic singularities but also by dynamic singularities [8], which are singularities due to the mass and inertia properties of the entire system. Dynamic singularities can occur if the generalized Jacobian matrix becomes singular [9]. As such, internal spacecraft control strategies have been proposed to mitigate both singularities [10].

Coordinated control, also referred to as free-flying spacecraft [6], consists of actuating the spacecraft base and manipulator simultaneously. This approach allows for planning of the joint trajectories independently from the motion of the base and is most applicable when there are pose constraints on the spacecraft base, such as antenna orientation for communication, or camera pointing for observation. Free-flying approaches, however, consume valuable resources, such as fuel.

Prior contributions to the field of coordinated control of SMRSs are numerous and worth expanding upon. In particular, the works of Carignan and Akin [11] present a generalizable set of equations of motion, along with a control strategy to stabilize a satellite base during manipulator tasks. However, that work did not address several complications, such as self-colliding base-manipulator configurations or translational constraints that may exist for both the spacecraft

base and manipulator(s). A coordinated control method that exhibits robustness with respect to the mass properties, as well as external disturbances, was proposed by Jayakody et al. [12], although this algorithm necessitated that all SMRS inertial maneuvers be manually planned and computed in advance.

In early studies, coordinated control for the SMRS was established for the spacecraft base and manipulator independently [6,9], necessitating inverse-kinematics/dynamics of the joint-space for control of the manipulator [8,10]. However, due to the dynamic coupling between the spacecraft base and the manipulator(s) resulting in undesired control interactions between the respective independent control systems [13,14], there has been a trend to move towards a more coordinated control approach to address the system as a whole [15]. Specifically, a control strategy for approaching and grasping a target spacecraft by considering the servicing SMRS spacecraft base and manipulator as a single multibody system was given in [16]. Similarly, a coordinated control procedure for end-effector tracking and base regulation, focusing on the effects of different sampling rates of the spacecraft base and manipulator, was presented in [17]. Moreover, Mishra et al. [18] developed a holistic coordinated control method for a fully actuated free-flying SMRS during the approach phase to a tumbling target that utilized a cascading interconnection of a geometric extended Kalman filter and a geometric controller.

Similarly to the previous approaches we also propose a coordinated control design for the whole SMRS, i.e., planning for both the spacecraft base and manipulator simultaneously. Contrary to the earlier results in this area, we use dual quaternions to model the whole SMRS system. Dual quaternions describe both rotational motion and translational motion of rigid bodies, and offer a comprehensive solution to 6-DOF spacecraft dynamic modeling [19,20], estimation [21], and controller design [22] problems. In particular, this paper uses recent advances in dual quaternion (6+N)-DOF multibody spacecraft modeling [23–26] to formulate a new single system coordinated control framework for SMRSs.

We argue that the compact representation of the dual quaternion formalism leads to a transparent and easy-to-derive control design. Specifically, the dual quaternion algebra can be readily formulated for coordinated control of SMRSs treated as a single multibody system via a compact Lyapunov analysis. We propose a hybrid nonlinear feedback controller for coordinated control of SMRSs using dual quaternion that achieves the following:

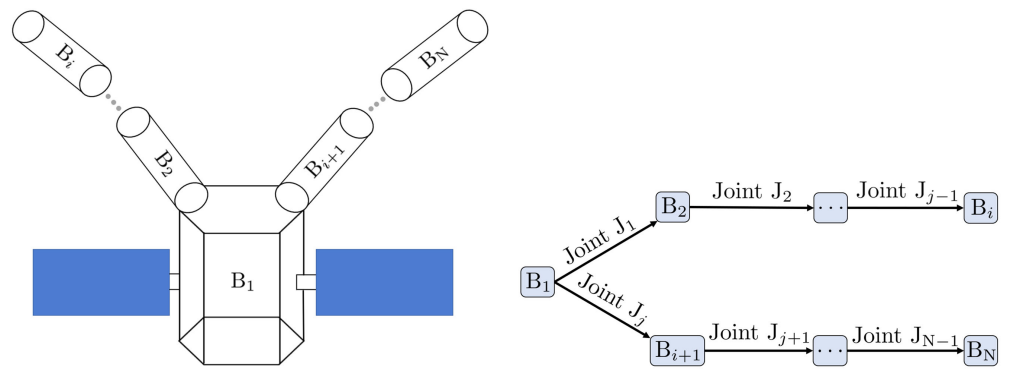
- 1) globally asymptotically stable pose tracking of both the spacecraft base and end effector(s) simultaneously,
- 2) robustness to chattering from feedback noise via a hybrid logic function [27,28], and
- 3) mitigating the unwinding phenomenon innate to continuousbased quaternion and consequentially dual quaternion controllers [29,30].

The proposed dual quaternion control law does not necessitate the inverse of joint kinematics during control design and additionally can be formulated to passively mitigate system singularities via actuator allocation, which may occur during the tracking maneuver, ensuring bounded control inputs, with minimum spacecraft base and endeffector deviation from the specified trajectories.

The rest of this paper is structured as follows: In Sec. II, we present how to use dual quaternions to represent and model multibody spacecraft systems. Section III proves the global asymptotic stability of the simultaneous spacecraft base and end-effector dual quaternion posetracking controller, while Sec. IV compliments the proposed controller with an actuator allocation technique for guaranteeing execution of the proposed control when there are no system singularities and minimizes tracking error in the neighborhood of singularities. Finally, Sec. V presents simulation results that verify the proposed controller and allocation performance and efficacy, and Sec. VI summarizes our concluding observations and future works.

II. Dual Quaternion Modeling of Multibody Spacecraft-Mounted Robotic Systems

This section establishes both the inertial and relative dual quaternion kinematic and dynamic modeling for SMRSs. The dual



a) A two-arm spacecraft-mounted robotic system

b) Two-arm SMRS as a rooted tree with vertices and edges

Fig. 1 N-body spacecraft-mounted robotic system description. Figure adapted from [26].

quaternion multibody kinematics and dynamics framework necessary to describe SMRSs is based on [23–25]. For a review of quaternion and dual quaternion algebras, as they pertain to rigid-body motion, the interested reader is referred to [26].

A. Multibody Kinematics

Consider the unit dual quaternion, describing both position and attitude or *pose*, of the rigid-body B given by

$$\mathbf{q}_{\mathcal{B}/\mathcal{I}} = q_{\mathcal{B}/\mathcal{I}} + \epsilon q_{\mathcal{B}/\mathcal{I}} r_{\mathsf{R}/\mathsf{O}}^{\mathcal{B}} \in \mathbb{H}_d^u \tag{1}$$

where ϵ is the *dual unit* defined by $\epsilon^2=0$ and $\epsilon\emptyset$, the quaternion $r_{\mathrm{B/O}}^{\mathcal{B}}=(0,\bar{r}_{\mathrm{B/O}}^{\mathcal{B}})\in\mathbb{H}^v$, with position vector $\bar{r}_{\mathrm{B/O}}^{\mathcal{B}}\in\mathbb{R}^3$ and the unit attitude quaternion, represented as the ordered pair, $q_{\mathcal{B/I}}=(q^0,\bar{q})\in\mathbb{H}^u$, where $\bar{q}=[q_1,q_2,q_3]^{\mathsf{T}}\in\mathbb{R}^3$ is the *vector part* of the quaternion and $q^0\in\mathbb{R}$ is the *scalar part* of the quaternion. Note that the dual quaternion given in Eq. (1) is unit dual quaternion, i.e., $q_{\mathcal{B/I}}=q_r+\epsilon q_d\in\mathbb{H}^u_d=\{q\in\mathbb{H}_d:q\cdot q=qq^*=q^*q=1\}$, as Eq. (1) satisfies the two algebraic constraints $q_r\cdot q_r=1$ and $q_r\cdot q_r=0$, where q_r , $q_r\in\mathbb{H}$ are the *real part* and the *dual part* of the dual quaternion, respectively. The accompanying dual velocity is given by

$$\boldsymbol{\omega}_{\mathcal{B}/\mathcal{I}}^{\mathcal{B}} = \left(0, \bar{\omega}_{\mathcal{B}/\mathcal{I}}^{\mathcal{B}}\right) + \epsilon \left(0, \bar{v}_{\mathsf{B}/\mathsf{O}}^{\mathcal{B}}\right) \in \mathbb{H}_{d}^{v} \tag{2}$$

where $\bar{\omega}_{B/\mathcal{I}}^{\mathcal{B}}$, $\bar{v}_{B/O}^{\mathcal{B}} \in \mathbb{R}^3$ are the angular and linear velocity vectors of body B, respectively, expressed in frame \mathcal{B} [20].

When we consider *N*-body SMRSs, like the one shown in Fig. 1, the kinematics of the system is described by the satellite base and the generalized joint coordinates, $\Gamma \triangleq [\Gamma_1 \cdots \Gamma_j \cdots \Gamma_{N-1}]^T \in \mathbb{R}^D$, of the manipulator(s), where $D = \sum_{j=1}^{N-1} d_j$, with d_j being the DOF of joint J_i and, as such, determines the form of Γ_i .

The joint dual velocity expressed in joint coordinates can be determined from

$$\boldsymbol{\omega}_{\mathcal{I}_{j}/\mathcal{B}_{i}}^{\mathcal{I}_{j}} = \boldsymbol{q}_{\mathcal{B}_{i+1}/\mathcal{I}_{j}} \boldsymbol{\omega}_{\mathcal{B}_{i+1}/\mathcal{I}}^{\mathcal{B}_{i+1}} \boldsymbol{q}_{\mathcal{B}_{i+1}/\mathcal{I}_{j}}^{*} - \boldsymbol{q}_{\mathcal{I}_{j}/\mathcal{B}_{i}}^{*} \boldsymbol{\omega}_{\mathcal{B}_{i}/\mathcal{I}}^{\mathcal{B}_{i}} \boldsymbol{q}_{\mathcal{I}_{j}/\mathcal{B}_{i}}$$
(3)

while the relationship between generalized speeds and dual velocities is given by

$$\dot{\Gamma}_{j} = \Pi_{j} \circledast \boldsymbol{\omega}_{\mathcal{I}_{j}/\mathcal{B}_{i}}^{\mathcal{I}_{j}} \tag{4}$$

where $\circledast: \mathbb{R}^{d_j \times 8} \times \mathbb{H}_d^v \to \mathbb{R}^{d_j}$ maps $\omega_{\mathcal{J}_j/\mathcal{B}_i}^{\mathcal{J}_j}$ via the projection matrix Π_j depending on the type of joint J_j , the exact expression of which is given in [23].

Therefore, given Eqs. (1), (2), and (4), the minimum state-space representation for *N*-body SMRSs is given by the pose of the

spacecraft base, $q_{\mathcal{B}_1/\mathcal{I}}$, the rates of that base, $\omega_{\mathcal{B}_1/\mathcal{I}}^{\mathcal{B}_1}$, the generalized joint coordinates, Γ , and their rates, $\dot{\Gamma}$, as shown below§:

$$\bar{x} = \begin{bmatrix} \left[\boldsymbol{q}_{\mathcal{B}_1/\mathcal{I}} \right]^{\mathsf{T}} & \Gamma^{\mathsf{T}} & \left(\bar{\boldsymbol{\omega}}_{\mathcal{B}_1/\mathcal{I}}^{\mathcal{B}_1} \right)^{\mathsf{T}} & \dot{\Gamma}^{\mathsf{T}} \end{bmatrix}^{\mathsf{T}} \in \mathbb{R}^8 \times \mathbb{R}^D \times \mathbb{R}^6 \times \mathbb{R}^D$$
(5)

B. Multibody Dynamics

Differentiating Eq. (1) results in the kinematic equations of motion for a unit dual quaternion as

$$\dot{\boldsymbol{q}}_{\mathcal{B}/\mathcal{I}} = \frac{1}{2} \boldsymbol{q}_{\mathcal{B}/\mathcal{I}} \boldsymbol{\omega}_{\mathcal{B}/\mathcal{I}}^{\mathcal{B}} \tag{6}$$

Taking the time derivative of $\omega_{\mathcal{B}/\mathcal{I}}^{\mathcal{B}}$ in Eq. (2) yields the compact representation of the Newton–Euler equations of motion for the rigid body in 6-DOF motion as [26]

$$M_{\rm B} \star \dot{\omega}_{\mathcal{B}/\mathcal{I}}^{\mathcal{B}} + \omega_{\mathcal{B}/\mathcal{I}}^{\mathcal{B}} \times \left(M_{\rm B} \star \omega_{\mathcal{B}/\mathcal{I}}^{\mathcal{B}} \right) = W_{\rm B,sum}^{\mathcal{B}}(O_{\mathcal{B}})$$
 (7)

where the operator \star denotes the multiplication of a dual quaternion with an 8-by-8 matrix, $W_{\mathrm{B,sum}}^{\mathcal{B}}(O_{\mathcal{B}}) = f^{\mathcal{B}} + \epsilon \tau^{\mathcal{B}}$ is the sum total dual wrench, i.e., the total force and torque applied about the center of mass of body B, given that $f^{\mathcal{B}} = (0, \bar{f}^{\mathcal{B}})$ and $\tau^{\mathcal{B}} = (0, \bar{\tau}^{\mathcal{B}})$, where $\bar{f}^{\mathcal{B}}$, $\bar{\tau}^{\mathcal{B}} \in \mathbb{R}^3$ are the applied forces and torques in frame \mathcal{B} , respectively, and M_{B} is dual inertia matrix comprising both the mass m_{B} and the inertia matrix \bar{I}_{B} of body B.

Applying Eq. (7) to the B_i th body of SMRSs and denoting T as the collection of all dual reaction wrenches from physical constraints between respective bodies, as

$$T = \left(\mathbf{W}_{B_{2}/B_{1}}^{\mathcal{J}_{1}}(O_{\mathcal{J}_{1}}) \cdots \mathbf{W}_{B_{i+1}/B_{i}}^{\mathcal{J}_{j}}(O_{\mathcal{J}_{j}}) \cdots \mathbf{W}_{B_{N}/B_{N-1}}^{\mathcal{J}_{N-1}}(O_{\mathcal{J}_{N-1}}) \right)$$
(8)

and letting v be the collection of all dual body velocities be

$$\boldsymbol{v} = \left(\boldsymbol{\omega}_{\mathcal{B}_1/\mathcal{I}}^{\mathcal{B}_1} \cdots \boldsymbol{\omega}_{\mathcal{B}_i/\mathcal{I}}^{\mathcal{B}_i} \cdots \boldsymbol{\omega}_{\mathcal{B}_N/\mathcal{I}}^{\mathcal{B}_N}\right) \tag{9}$$

then we can obtain a compact form for the Newton-Euler equations of motion of SMRSs as

$$\begin{bmatrix} \mathbf{S}_{11} & \mathbf{S}_{12} \\ \mathbf{S}_{21} & \bar{\mathbf{0}} \end{bmatrix} \star \begin{bmatrix} \dot{\boldsymbol{v}} \\ \mathbf{T} \end{bmatrix} = \begin{bmatrix} \mathbf{Q}_1 \\ \mathbf{Q}_2 \end{bmatrix}$$
 (10)

^{*}For more details, refer to Lemma 58 in [20].

 $[\]S[\cdot]: \mathbb{H}_d \to \mathbb{R}^8$ is the bijective mapping between the set of dual quaternions and \mathbb{R}^8 , and $\overline{\cdot}: \mathbb{H}_d^v \to \mathbb{R}^6$ removes the zeros from a vector dual quaternion (for details see [19]).

where $S_{11} = \text{blkdiag}(M_{B_1} \cdots M_{B_N})$ consists of the dual inertia matrix for each of the bodies, and where the matrices S_{12} and S_{21} contain the coordinate transformations of the unknown reaction wrenches that appear in the Newton–Euler equations and of the dual accelerations of each body from the joint constraint equations, respectively.

The vector Q_1 is composed of a collection of subvectors, one for each B_i th body:

$$(Q_{1})_{i} = -\boldsymbol{\omega}_{\mathcal{B}_{i}/\mathcal{I}}^{\mathcal{B}_{i}} \times \left(M_{\mathbf{B}_{i}} \star \boldsymbol{\omega}_{\mathcal{B}_{i}/\mathcal{I}}^{\mathcal{B}_{i}} \right) + \boldsymbol{W}_{\mathbf{B}_{i}}^{\mathcal{B}_{i}} (O_{\mathcal{B}_{i}})$$

$$+ \sum_{i=1}^{N-1} C_{ij} \boldsymbol{q}_{\mathcal{I}_{j}/\mathcal{B}_{i}} \boldsymbol{W}_{\mathbf{J}_{j,act}}^{\mathcal{J}_{j}} (O_{\mathcal{J}_{j}}) \boldsymbol{q}_{\mathcal{J}_{j}/\mathcal{B}_{i}}^{*}$$

$$(11)$$

where $W_{\mathbf{J}_{j},\mathrm{act}}^{\mathcal{J}_{j}}(O_{\mathcal{J}_{j}})$ is the actuation wrench about the DOF of joint \mathbf{J}_{j} ; $W_{\mathbf{B}_{i}}^{\mathcal{B}_{i}}(O_{\mathcal{B}_{i}})$ arises due to other environmental external sources, such as solar pressure, or gravity gradients; and the components of adjacency matrix C_{ij} , describing the connectivity of the bodies and joints of SMRSs, are used to appropriately assign the correct signs to the respective actuation wrenches per body. The vector \mathbf{Q}_{2} corresponds to the right-hand side of the kinematic constraint equations for each of the \mathbf{J}_{j} joints, such that

$$(\mathbf{Q}_{2})_{i} = \boldsymbol{q}_{\mathcal{J}_{i}/\mathcal{B}_{i}}^{*} \boldsymbol{\omega}_{\mathcal{B}_{i}/\mathcal{I}}^{\mathcal{B}_{i}} \boldsymbol{q}_{\mathcal{J}_{i}/\mathcal{B}_{i}} \times \boldsymbol{\omega}_{\mathcal{J}_{i}/\mathcal{B}_{i}}^{\mathcal{J}_{j}}$$
(12)

Given Eq. (10), it follows that

$$\dot{\boldsymbol{v}} = S_{11}^{-1}(Q_1 - S_{12} \star T) \quad \text{and} \quad T = \left(S_{21}S_{11}^{-1}S_{12}\right)^{-1}\left(S_{21}S_{11}^{-1}Q_1 - Q_2\right)$$
(13)

The derivative of $\dot{\Gamma}$ from Eq. (4) leads to

$$\ddot{\Gamma}_{j} = \dot{\Pi}_{j} \otimes \boldsymbol{\omega}_{\mathcal{I}_{i}/\mathcal{B}_{i}}^{\mathcal{I}_{j}} + \Pi_{j} \otimes \dot{\boldsymbol{\omega}}_{\mathcal{I}_{i}/\mathcal{B}_{i}}^{\mathcal{I}_{j}}$$

$$\tag{14}$$

where by differentiating $\boldsymbol{\omega}_{\mathcal{J}_j/\mathcal{B}_i}^{\mathcal{J}_j}$ from Eq. (3), given the solution of dual accelerations, $\dot{\boldsymbol{v}}$, from Eq. (13), yields

$$\dot{\boldsymbol{\omega}}_{\mathcal{J}_{j}/\mathcal{B}_{i}}^{\mathcal{J}_{j}} = \boldsymbol{q}_{\mathcal{B}_{i+1}/\mathcal{J}_{j}} \dot{\boldsymbol{\omega}}_{\mathcal{B}_{i+1}/\mathcal{I}}^{\mathcal{B}_{i+1}} \boldsymbol{q}_{\mathcal{B}_{i+1}/\mathcal{J}_{j}}^{*} - \boldsymbol{q}_{\mathcal{J}_{j}/\mathcal{B}_{i}}^{*} \left(\dot{\boldsymbol{\omega}}_{\mathcal{B}_{i}/\mathcal{I}}^{\mathcal{B}_{i}} + \boldsymbol{\omega}_{\mathcal{B}_{1}/\mathcal{I}}^{\mathcal{B}_{i}} \times \boldsymbol{\omega}_{\mathcal{J}_{j}/\mathcal{B}_{i}}^{\mathcal{B}_{i}} \right) \boldsymbol{q}_{\mathcal{J}_{j}/\mathcal{B}_{i}}$$
(15)

Finally, given Eqs. (4), (6), (13), and (14), we can express the time derivative of the system state \bar{x} in Eq. (5) as

$$\dot{\bar{x}} = \begin{bmatrix} \left[\dot{\boldsymbol{q}}_{\mathcal{B}_1/\mathcal{I}} \right]^{\mathsf{T}} & \dot{\Gamma}^{\mathsf{T}} & \left(\dot{\bar{\boldsymbol{\omega}}}_{\mathcal{B}_1/\mathcal{I}}^{\mathcal{B}_1} \right)^{\mathsf{T}} & \ddot{\Gamma}^{\mathsf{T}} \end{bmatrix}^{\mathsf{T}}$$
(16)

C. End-Effector Kinematics and Dynamics of Spacecraft Manipulators

To determine the inertial pose, rates, and accelerations of the end effector during control design, we proceed as follows. Given Eq. (5), the pose of the end effector(s) of SMRSs is given by the following kinematic relationship:

$$\boldsymbol{q}_{\mathcal{G}/\mathcal{I}} = \boldsymbol{q}_{\mathcal{B}_1/\mathcal{I}} \boldsymbol{q}_{\mathcal{J}_j/\mathcal{B}_i} \boldsymbol{q}_{\mathcal{B}_{i+1}/\mathcal{J}_j} \cdots \boldsymbol{q}_{\mathcal{J}_{N-1}/\mathcal{B}_{N-1}} \boldsymbol{q}_{\mathcal{B}_N/\mathcal{J}_{N-1}} \boldsymbol{q}_{\mathcal{G}/\mathcal{B}_N}$$
(17)

where $q_{\mathcal{G}/\mathcal{I}}$ is the inertial end-effector pose and where $q_{\mathcal{J}_j/\mathcal{B}_i}$ are state-dependent dual quaternions constructed from Γ_j [24]. Note that because the end effector frame \mathcal{G} is rigidly attached to body \mathcal{B}_N , the time derivative of Eq. (17) simplifies to the following:

$$\boldsymbol{\omega}_{\mathcal{G}/\mathcal{I}}^{\mathcal{G}} = \boldsymbol{q}_{\mathcal{G}/\mathcal{B}_{N}}^{*} \boldsymbol{\omega}_{\mathcal{B}_{N}/\mathcal{I}}^{\mathcal{B}_{N}} \boldsymbol{q}_{\mathcal{G}/\mathcal{B}_{N}}$$
(18)

The time derivative of Eq. (18) yields the end-effector dual acceleration, $\dot{\omega}_{\mathcal{G}/\mathcal{I}}^{\mathcal{G}} \in \mathbb{H}_d^v$,

$$\dot{\boldsymbol{\omega}}_{\mathcal{G}/\mathcal{I}}^{\mathcal{G}} = \boldsymbol{q}_{\mathcal{G}/\mathcal{B}_{N}}^{*} \dot{\boldsymbol{\omega}}_{\mathcal{B}_{N}/\mathcal{I}}^{\mathcal{B}_{N}} \boldsymbol{q}_{\mathcal{G}/\mathcal{B}_{N}}$$
(19)

D. Expressing the Control of SMRSs

For reasons that will become evident during controller design, we rearrange the form of $\dot{\boldsymbol{v}}$ from Eq. (10) such that the SMRS collection of dual actuation wrenches is expressed as

$$\mathbf{u} = \left(\mathbf{W}_{\mathrm{B}_{1},\mathrm{act}}^{\mathcal{B}_{1}}(O_{\mathcal{B}_{1}}) \quad \mathbf{W}_{\mathrm{J}_{1},\mathrm{act}}^{\mathcal{J}_{1}}(O_{\mathcal{J}_{1}}) \quad \cdots \quad \mathbf{W}_{\mathrm{J}_{\mathrm{N-1}},\mathrm{act}}^{\mathcal{J}_{\mathrm{N-1}}}(O_{\mathcal{J}_{\mathrm{N-1}}}) \right)$$

$$\in \mathbb{H}_{d}^{\nu} \times \mathbb{H}_{d}^{\nu} \times \cdots \times \mathbb{H}_{d}^{\nu}$$
(20)

where $W_{\mathrm{B}_{1},\mathrm{act}}^{\mathcal{B}_{1}}(O_{\mathcal{B}_{1}})$ is the actuation wrench applied on the spacecraft base (obtained from firing thrusters and actuating momentum exchange devices) and $W_{\mathrm{J}_{j},\mathrm{act}}^{\mathcal{J}_{j}}(O_{\mathcal{J}_{j}})$ is the actuation wrench of the J_{i} joint of the manipulator(s).

Re-arranging Eq. (10), $\dot{\boldsymbol{v}}$ can be expressed as

$$\dot{\boldsymbol{v}} = S_{11}^{-1} \left(I_{8\times8} - S_{12} \left(S_{21} S_{11}^{-1} S_{12} \right)^{-1} S_{21} S_{11}^{-1} \right) Q_1$$

$$+ S_{11}^{-1} S_{12} \left(S_{21} S_{11}^{-1} S_{12} \right)^{-1} Q_2$$
(21)

To explicitly express the control vector \boldsymbol{u} in Eq. (21), we decompose Q_1 so that $Q_1 = Q_{1,\text{non-act}} + Q_{1,\text{act}}$, where $Q_{1,\text{non-act}}$ contains the nonlinear terms and external forces applied to each body given by

$$(Q_{1,\text{non-act}})_{i} = -\boldsymbol{\omega}_{\mathcal{B}_{i}/\mathcal{I}}^{\mathcal{B}_{i}} \times \left(M_{B_{i}} \star \boldsymbol{\omega}_{\mathcal{B}_{i}/\mathcal{I}}^{\mathcal{B}_{i}} \right) + W_{B_{i}}^{\mathcal{B}_{i}}(O_{\mathcal{B}_{i}})$$
(22)

and $\mathtt{Q}_{1,\text{act}}$ contains all of the control dual wrenches of the system and is given by

$$(Q_{1,\text{act}})_i = b_i \boldsymbol{W}_{B_1,\text{act}}^{\mathcal{B}_1}(O_{\mathcal{B}_1}) + \sum_{j=1}^{N-1} C_{ij} \boldsymbol{q}_{\mathcal{J}_j/\mathcal{B}_i} \boldsymbol{W}_{J_j,\text{act}}^{\mathcal{J}_j}(O_{\mathcal{J}_j}) \boldsymbol{q}_{\mathcal{J}_j/\mathcal{B}_i}^*$$
(23)

where $b_i = \{1, 0, \dots, 0\}$ selects the actuation wrench for the spacecraft base on only the first body. Furthermore, we express $Q_{1,act} = Q_u \star u$, where $Q_u \in \mathbb{R}^{8N \times 8N}$ is given by

$$Q_{u} = \begin{bmatrix} I_{8\times8} & -Q_{R}(\boldsymbol{q}_{\mathcal{J}_{J}/\mathcal{B}_{i}}^{*}) & \bar{0}_{8\times8} & \cdots & \bar{0}_{8\times8} & \bar{0}_{8\times8} \\ \bar{0}_{8\times8} & Q_{L}(\boldsymbol{q}_{\mathcal{B}_{i+1}/\mathcal{J}_{j}}^{*}) & -Q_{R}(\boldsymbol{q}_{\mathcal{J}_{j+1}/\mathcal{B}_{i+1}}^{*}) & \cdots & \bar{0}_{8\times8} & \bar{0}_{8\times8} \\ \vdots & \vdots & \vdots & \ddots & \vdots & \vdots \\ \bar{0}_{8\times8} & \bar{0}_{8\times8} & \bar{0}_{8\times8} & \cdots & Q_{L}(\boldsymbol{q}_{\mathcal{B}_{N-1}/\mathcal{J}_{N-2}}^{*}) & -Q_{R}(\boldsymbol{q}_{\mathcal{J}_{N-1}/\mathcal{B}_{N-1}}^{*}) \\ \bar{0}_{8\times8} & \bar{0}_{8\times8} & \bar{0}_{8\times8} & \cdots & \bar{0}_{8\times8} & Q_{L}(\boldsymbol{q}_{\mathcal{B}_{N}/\mathcal{J}_{N-1}}^{*}) \end{bmatrix}$$

$$(24)$$

[¶] For the details on the construction of S_{21} and S_{12} in Eq. (10), refer to [24].

where, given dual quaternion $\mathbf{q} = q_r + \epsilon q_d$, the matrices $Q_L(\mathbf{q}^*) = Q_R(\mathbf{q}) = [\![\mathbf{q}^*]\!]_L [\![\mathbf{q}]\!]_R$ are shorthand for the multiplication of the left and right dual quaternion multiplication operators $[\![\cdot]\!]_L$, $[\![\cdot]\!]_R : \mathbb{H}_d \to \mathbb{R}^{8\times 8}$ defined as [25]

$$[\![\boldsymbol{q}]\!]_{L} = \begin{bmatrix} [q_r]_{L} & \bar{0}_{4\times4} \\ [q_d]_{L} & [q_r]_{L} \end{bmatrix} \quad \text{and} \quad [\![\boldsymbol{q}]\!]_{R} = \begin{bmatrix} [q_r]_{R} & \bar{0}_{4\times4} \\ [q_d]_{R} & [q_r]_{R} \end{bmatrix} \tag{25}$$

given that for quaternion $q=(q^0,\bar{q})$, the left and right quaternion multiplication operators $[\cdot]_L,[\cdot]_R:\mathbb{H}\to\mathbb{R}^{4\times 4}$ are given as

$$[q]_{L} = \begin{bmatrix} q^{0} & -\bar{q}^{\mathsf{T}} \\ \bar{q} & q^{0}I_{3\times3} + [\bar{q}]^{\mathsf{X}} \end{bmatrix} \quad \text{and} \quad [q]_{R} = \begin{bmatrix} q^{0} & -\bar{q}^{\mathsf{T}} \\ \bar{q} & q^{0}I_{3\times3} - [\bar{q}]^{\mathsf{X}} \end{bmatrix}$$
(26)

where $[\cdot]^{\times}: \mathbb{R}^3 \to \mathbb{R}^{3\times 3}$ is the skew-symmetric matrix operator of the vector part of the quaternion, i.e.,

$$[\bar{q}]^{\times} = \begin{bmatrix} 0 & -q_3 & q_2 \\ q_3 & 0 & -q_1 \\ -q_2 & q_1 & 0 \end{bmatrix}$$
 (27)

Decomposing Q_1 allows for Eq. (21) to be expressed as

$$\dot{\boldsymbol{v}} = \Phi(\bar{x}) + \Psi(\bar{x}) \star \boldsymbol{u} \tag{28}$$

where $\Phi(\bar{x}) \in \mathbb{R}^{8N}$ is given by

$$\Phi(\bar{x}) = S_{11}^{-1} \Big(I_{8\times8} - S_{12} \Big(S_{21} S_{11}^{-1} S_{12} \Big)^{-1} S_{21} S_{11}^{-1} \Big) Q_{1,\text{non-act}}
+ S_{11}^{-1} S_{12} \Big(S_{21} S_{11}^{-1} S_{12} \Big)^{-1} Q_{2}$$
(29)

and where $\Psi(\bar{x}) \in \mathbb{R}^{8N \times 8N}$ is given by

$$\Psi(\bar{x}) = S_{11}^{-1} \left(I_{8\times8} - S_{12} \left(S_{21} S_{11}^{-1} S_{12} \right)^{-1} S_{21} S_{11}^{-1} \right) Q_u$$
 (30)

E. Relative Dual Quaternion Equations of Motion

Given two desired time-varying reference frames, one for the end effector denoted by $\mathcal E$ and one for the base of the spacecraft denoted

From the transport theorem, it follows that $\dot{\omega}_{\mathcal{E}/\mathcal{I}}^{\mathcal{G}}$, and $\dot{\omega}_{\mathcal{S}/\mathcal{I}}^{\mathcal{B}_1}$ are given by

$$\dot{\boldsymbol{\omega}}_{\mathcal{E}/\mathcal{I}}^{\mathcal{G}} = \boldsymbol{q}_{\mathcal{G}/\mathcal{E}}^{*} \left(\dot{\boldsymbol{\omega}}_{\mathcal{E}/\mathcal{I}}^{\mathcal{E}} - \boldsymbol{\omega}_{\mathcal{G}/\mathcal{E}}^{\mathcal{E}} \times \boldsymbol{\omega}_{\mathcal{E}/\mathcal{I}}^{\mathcal{E}} \right) \boldsymbol{q}_{\mathcal{G}/\mathcal{E}} \quad \text{and}$$

$$\dot{\boldsymbol{\omega}}_{\mathcal{S}/\mathcal{I}}^{\mathcal{B}_{1}} = \boldsymbol{q}_{\mathcal{B}_{1}/\mathcal{S}}^{*} \left(\dot{\boldsymbol{\omega}}_{\mathcal{S}/\mathcal{I}}^{\mathcal{S}} - \boldsymbol{\omega}_{\mathcal{B}_{1}/\mathcal{S}}^{\mathcal{S}} \times \boldsymbol{\omega}_{\mathcal{S}/\mathcal{I}}^{\mathcal{S}} \right) \boldsymbol{q}_{\mathcal{B}_{1}/\mathcal{S}}$$
(34)

Given the dynamics of each rigid body and the end effector of an SMRS in Eqs. (19) and (28), respectively, we express the spacecraft base dynamics as

$$\dot{\boldsymbol{\omega}}_{\mathcal{B}_1/\mathcal{I}}^{\mathcal{B}_1} = \boldsymbol{\Phi}_1(\bar{x}) + \boldsymbol{\Psi}_1(\bar{x}) \star \boldsymbol{u}_{\mathbf{B}_1} \tag{35}$$

and the end-effector dynamics as

$$\dot{\boldsymbol{\omega}}_{\mathcal{G}/\mathcal{I}}^{\mathcal{G}} = \boldsymbol{q}_{\mathcal{G}/\mathcal{B}_{N}}^{*} \left(\Phi_{N}(\bar{x}) + \Psi_{N}(\bar{x}) \star \boldsymbol{u}_{J_{1:N}} \right) \boldsymbol{q}_{\mathcal{G}/\mathcal{B}_{N}}$$
(36)

where $u = (u_{B_1}, u_{J_{1:N}})$, where u_{B_1} and $u_{J_{1:N}}$ are the wrenches generated from the base and manipulator, respectively.

III. Simultaneous Multibody Spacecraft Manipulator Control Law

In this section, we derive a robust to feedback-noise-induced chattering hybrid globally asymptotically stable feedback controller for simultaneous pose tracking of the spacecraft base and end effector of nonredundant and redundant multibody SMRSs. Note that, for simplicity, we derive the control law considering an SMRS with a single manipulator, but the resulting controller is easily extendable to systems with more than one manipulator.

When the relative linear and angular velocities of the spacecraft base and the end effector with respect to the desired velocities are known, a globally asymptotically stable, time-varying, pose-tracking nonlinear control law for both the spacecraft base and the end effector of SRMSs that is robust-to-chattering because of process noise can be constructed as follows.

Let matrices $K_{\mathcal{B}_1}$, $K_{\mathcal{G}} > 0$, and scalars $p_{\mathcal{B}_1}$, $p_{\mathcal{G}}$, $k_{\mathcal{B}_1}$, $k_{\mathcal{G}} > 0$, and consider the following feedback control law:

$$\Psi_{1,N}(\bar{x}) \star \boldsymbol{u} = \begin{bmatrix} -\Phi_{1}(\bar{x}) + \dot{\boldsymbol{\omega}}_{S/\mathcal{I}}^{\mathcal{B}_{1}} + S(K_{\mathcal{B}_{1}}^{-1}) \star \left[-k_{\mathcal{B}_{1}} \boldsymbol{\omega}_{\mathcal{B}_{1}/S}^{\mathcal{B}_{1}} - p_{\mathcal{B}_{1}} \operatorname{vec} \left(\boldsymbol{q}_{\mathcal{B}_{1}/S}^{*} \left(\boldsymbol{q}_{\mathcal{B}_{1}/S} - \alpha \left(q_{\mathcal{B}_{1}/S,r}^{0} \right) \mathbf{1} \right)^{s} \right)^{s} \right] \\ -\Phi_{N}(\bar{x}) + \boldsymbol{q}_{\mathcal{G}/\mathcal{B}_{N}} \left(\dot{\boldsymbol{\omega}}_{\mathcal{E}/\mathcal{I}}^{\mathcal{G}} + S(K_{\mathcal{G}}^{-1}) \star \left[-k_{\mathcal{G}} \boldsymbol{\omega}_{\mathcal{G}/\mathcal{E}}^{\mathcal{G}} - p_{\mathcal{G}} \operatorname{vec} \left(\boldsymbol{q}_{\mathcal{G}/\mathcal{E}}^{*} \left(\boldsymbol{q}_{\mathcal{G}/\mathcal{E}} - \alpha \left(q_{\mathcal{G}/\mathcal{E},r}^{0} \right) \mathbf{1} \right)^{s} \right)^{s} \right] \right) \boldsymbol{q}_{\mathcal{G}/\mathcal{B}_{N}}^{*} \end{bmatrix}$$

$$(37)$$

by S, we can express the corresponding relative error poses as

$$q_{\mathcal{G}/\mathcal{E}} = q_{\mathcal{E}/\mathcal{I}}^* q_{\mathcal{G}/\mathcal{I}}$$
 and $q_{\mathcal{B}_1/\mathcal{S}} = q_{\mathcal{S}/\mathcal{I}}^* q_{\mathcal{B}_1/\mathcal{I}}$ (31)

Thus, the derivative of Eq. (31) determines the relative kinematics between the desired frames of the spacecraft base and end effector, respectively, as

$$\dot{\boldsymbol{q}}_{\mathcal{G}/\mathcal{E}} = \frac{1}{2} \boldsymbol{q}_{\mathcal{G}/\mathcal{E}} \boldsymbol{\omega}_{\mathcal{G}/\mathcal{E}}^{\mathcal{G}} \quad \text{and} \quad \dot{\boldsymbol{q}}_{\mathcal{B}_1/\mathcal{S}} = \frac{1}{2} \boldsymbol{q}_{\mathcal{B}_1/\mathcal{S}} \boldsymbol{\omega}_{\mathcal{B}_1/\mathcal{S}}^{\mathcal{B}_1}$$
 (32)

where the relative dual velocities are $\boldsymbol{\omega}_{\mathcal{G}/\mathcal{E}}^{\mathcal{G}} = \boldsymbol{\omega}_{\mathcal{G}/\mathcal{I}}^{\mathcal{G}} - \boldsymbol{\omega}_{\mathcal{E}/\mathcal{I}}^{\mathcal{G}}$, and $\boldsymbol{\omega}_{\mathcal{B}_{1}/\mathcal{S}}^{\mathcal{B}_{1}} = \boldsymbol{\omega}_{\mathcal{B}_{1}/\mathcal{I}}^{\mathcal{B}_{1}} - \boldsymbol{\omega}_{\mathcal{S}/\mathcal{I}}^{\mathcal{B}_{1}}$.

Additionally, we express the relative dual acceleration of the end effector and the satellite base with respect to the desired reference frames \mathcal{E} and \mathcal{S} as

$$\dot{\boldsymbol{\omega}}_{\mathcal{G}/\mathcal{E}}^{\mathcal{G}} = \dot{\boldsymbol{\omega}}_{\mathcal{G}/\mathcal{I}}^{\mathcal{G}} - \dot{\boldsymbol{\omega}}_{\mathcal{E}/\mathcal{I}}^{\mathcal{G}} \quad \text{and} \quad \dot{\boldsymbol{\omega}}_{\mathcal{B}_{1}/\mathcal{S}}^{\mathcal{B}_{1}} = \dot{\boldsymbol{\omega}}_{\mathcal{B}_{1}/\mathcal{I}}^{\mathcal{B}_{1}} - \dot{\boldsymbol{\omega}}_{\mathcal{S}/\mathcal{I}}^{\mathcal{B}_{1}}$$
(33)

where we define $S(\cdot): \mathbb{R}^{8\times 8} \to \mathbb{R}^{8\times 8}$, such that, if $\mathbf{a} \in \mathbb{H}_d$ and $T \in \mathbb{R}^{8\times 8}$, then $(S(T) \star \mathbf{a})^{\mathrm{s}} = T \star (\mathbf{a})^{\mathrm{s}}$, and where $\mathrm{vec}(\mathbf{a}) = \mathrm{vec}(a_{\mathrm{r}}) + \epsilon \mathrm{vec}(a_{\mathrm{d}})$, given $\mathrm{vec}(a) = (0, \bar{a}) \in \mathbb{H}^v$ and the matrix $\Psi_{1,\mathrm{N}}(\bar{x}) = [\Psi_1(\bar{x}), \Psi_{\mathrm{N}}(\bar{x})]^{\mathsf{T}}$ is determined from Eqs. (35) and (36).

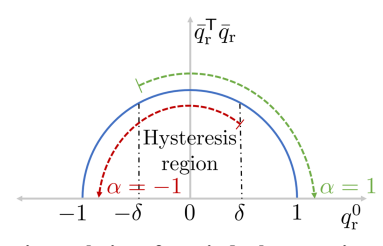


Fig. 2 Hysteretic regulation of a unit dual quaternion $q=q_{\rm r}+\epsilon q_{\rm d}$ to the set $\{\pm 1\}$. The state space for the real quaternion $q_{\rm r}$ of the dual quaternions is represented by the semicircle. The value of α determines if q should be regulated to 1 or -1. The parameter δ determines the hysteresis half-width [28].

Let also $\alpha(\cdot) \in \{-1, 1\}$ be a scalar *dynamic* memory state function that selects which pole of \mathbb{H}^u_d to regulate in a *hysteretic* fashion, inspired from the work from [28,31,32], as illustrated in Fig. 2. Specifically, letting $\delta \in (0,1)$ denote the hysteresis half-width, we define $\overline{\mathrm{sgn}}: \mathbb{R} \rightrightarrows \{-1,1\}$ as the outer semicontinuous set-valued map:

$$\overline{\text{sgn}}(s) = \begin{cases} sgn(s), & ||s|| > 0 \\ \{-1, 1\}, & s = 0, \end{cases} \text{ given } sgn(s) = \begin{cases} -1 & s < 0 \\ 1 & s \ge 0 \end{cases}$$
(38)

then the dynamics of α are governed by

$$\dot{\alpha} = 0$$
 when $q_{\rm r}^0 \alpha \ge -\delta$

$$\alpha^+ \in \overline{\rm sgn}(q_{\rm r}^0) \quad \text{when } q_{\rm r}^0 \alpha \le -\delta$$
 (39)

$$\dot{V} = \left(\boldsymbol{\omega}_{\mathcal{B}_{1}/\mathcal{S}}^{\mathcal{B}_{1}}\right)^{s} \circ \left(K_{\mathcal{B}_{1}} \star \left(\dot{\boldsymbol{\omega}}_{\mathcal{B}_{1}/\mathcal{S}}^{\mathcal{B}_{1}}\right)^{s}\right) + 2p_{\mathcal{B}_{1}}(\boldsymbol{q}_{\mathcal{B}_{1}/\mathcal{S}} - 1) \circ \dot{\boldsymbol{q}}_{\mathcal{B}_{1}/\mathcal{S}}
+ \left(\boldsymbol{\omega}_{\mathcal{G}/\mathcal{E}}^{\mathcal{G}}\right)^{s} \circ \left(K_{\mathcal{G}} \star \left(\dot{\boldsymbol{\omega}}_{\mathcal{G}/\mathcal{E}}^{\mathcal{G}}\right)^{s}\right) + 2p_{\mathcal{G}}(\boldsymbol{q}_{\mathcal{G}/\mathcal{E}} - 1) \circ \dot{\boldsymbol{q}}_{\mathcal{G}/\mathcal{E}} \tag{43}$$

Given that if $a, b, c \in \mathbb{H}_d$, then $a \circ (bc) = (b)^s \circ ((a)^s c^*) = (c)^s \circ (b^*(a)^s)$ [19], which implies that Eq. (43) can be expressed as

$$\dot{V} = \left(\boldsymbol{\omega}_{\mathcal{B}_{1}/\mathcal{S}}^{\mathcal{B}_{1}}\right)^{s} \circ \left(K_{\mathcal{B}_{1}} \star \left(\dot{\boldsymbol{\omega}}_{\mathcal{B}_{1}/\mathcal{I}}^{\mathcal{B}_{1}} - \dot{\boldsymbol{\omega}}_{\mathcal{S}/\mathcal{I}}^{\mathcal{B}_{1}}\right)^{s} + p_{\mathcal{B}_{1}} \boldsymbol{q}_{\mathcal{B}_{1}/\mathcal{S}}^{*} (\boldsymbol{q}_{\mathcal{B}_{1}/\mathcal{S}} - \mathbf{1})^{s}\right)
+ \left(\boldsymbol{\omega}_{\mathcal{G}/\mathcal{E}}^{\mathcal{G}}\right)^{s} \circ \left(K_{\mathcal{G}} \star \left(\dot{\boldsymbol{\omega}}_{\mathcal{G}/\mathcal{I}}^{\mathcal{G}} - \dot{\boldsymbol{\omega}}_{\mathcal{E}/\mathcal{I}}^{\mathcal{G}}\right)^{s} + p_{\mathcal{G}} \boldsymbol{q}_{\mathcal{G}/\mathcal{E}}^{*} (\boldsymbol{q}_{\mathcal{G}/\mathcal{E}} - \mathbf{1})^{s}\right)$$
(44)

Given the relative dual quaternion equations of motion in Eqs. (32) and (33), we can express Eq. (44) as

$$\dot{V} = \begin{bmatrix} \left(\boldsymbol{\omega}_{\mathcal{B}_{1}/\mathcal{S}}^{\mathcal{B}_{1}}\right)^{s} \\ \left(\boldsymbol{\omega}_{\mathcal{G}/\mathcal{E}}^{\mathcal{G}}\right)^{s} \end{bmatrix}^{\mathsf{T}} \circ \begin{bmatrix} p_{\mathcal{B}_{1}}\boldsymbol{q}_{\mathcal{B}_{1}/\mathcal{S}}^{*}(\boldsymbol{q}_{\mathcal{B}_{1}/\mathcal{S}} - \mathbf{1})^{s} + K_{\mathcal{B}_{1}} \star \left(\boldsymbol{\Phi}_{1}(\bar{x}) + \boldsymbol{\Psi}_{1}(\bar{x}) \star \boldsymbol{u}_{\mathbf{B}_{1}} - \dot{\boldsymbol{\omega}}_{\mathcal{S}/\mathcal{I}}^{\mathcal{B}_{1}}\right)^{s} \\ p_{\mathcal{G}}\boldsymbol{q}_{\mathcal{G}/\mathcal{E}}^{*}(\boldsymbol{q}_{\mathcal{G}/\mathcal{E}} - \mathbf{1})^{s} + K_{\mathcal{G}} \star \left(\boldsymbol{q}_{\mathcal{G}/\mathcal{B}_{N}}^{*}(\boldsymbol{\Phi}_{N}(\bar{x}) + \boldsymbol{\Psi}_{N}(\bar{x}) \star \boldsymbol{u}_{\mathbf{J}_{1:N}}\right)\boldsymbol{q}_{\mathcal{G}/\mathcal{B}_{N}} - \dot{\boldsymbol{\omega}}_{\mathcal{E}/\mathcal{I}}^{\mathcal{G}}\right)^{s} \end{bmatrix}$$

$$(45)$$

where α^+ denotes the value of the scalar logic function after being updated and q_r^0 is the scalar component of the real quaternion component of the dual quaternion $\mathbf{q} = q_r + \epsilon q_d$.

Theorem 1: Consider the rigid-body relative kinematic and dynamic equations given by Eqs. (32) and (33), respectively. Assuming that $q_{S/\mathcal{I}}, \omega_{S/\mathcal{I}}^{\mathcal{S}}, \dot{\omega}_{S/\mathcal{I}}^{\mathcal{S}}, q_{\mathcal{E}/\mathcal{I}}, \omega_{\mathcal{E}/\mathcal{I}}^{\mathcal{E}}, \dot{\omega}_{\mathcal{E}/\mathcal{I}}^{\mathcal{E}} \in \mathcal{L}_{\infty}^{**}$, and assuming that the dynamics matrix $\Psi(\bar{x})_{1,N}$ can be allocated such that, $\Phi_1(\bar{x})$, $\Phi_N(\bar{x}) \in \mathcal{L}_{\infty}$, then the control law in Eq. (37) results in $q_{\mathcal{B}_1/\mathcal{S}}(t) \to \pm 1$, $q_{\mathcal{G}/\mathcal{E}}(t) \to \pm 1$, $\omega_{\mathcal{B}_1/\mathcal{S}}^{\mathcal{B}_1}(t) \to 0$, and $\omega_{\mathcal{G}/\mathcal{E}}^{\mathcal{G}}(t) \to 0$ as $t \to \infty$ for any initial conditions.

Proof: Consider the following candidate Lyapunov function for the equilibrium point $q_{\mathcal{G}/\mathcal{E}} = 1$, $\omega_{\mathcal{G}/\mathcal{E}}^{\mathcal{G}} = 0$, $q_{\mathcal{B}_1/\mathcal{S}} = 1$, and $\omega_{\mathcal{B}_1/\mathcal{S}}^{\mathcal{B}_1} = 0$ of the closed-loop system formed by Eqs. (32), (33), and (37):

$$V\left(\boldsymbol{q}_{\mathcal{B}_{1}/\mathcal{S}}, \boldsymbol{\omega}_{\mathcal{B}_{1}/\mathcal{S}}^{\mathcal{B}_{1}}, \boldsymbol{q}_{\mathcal{G}/\mathcal{E}}, \boldsymbol{\omega}_{\mathcal{G}/\mathcal{E}}^{\mathcal{G}}\right)$$

$$= \frac{1}{2} \left(\boldsymbol{\omega}_{\mathcal{B}_{1}/\mathcal{S}}^{\mathcal{B}_{1}}\right)^{s} \circ \left(K_{\mathcal{B}_{1}} \star \left(\boldsymbol{\omega}_{\mathcal{B}_{1}/\mathcal{S}}^{\mathcal{B}_{1}}\right)^{s}\right) + p_{\mathcal{B}_{1}}(\boldsymbol{q}_{\mathcal{B}_{1}/\mathcal{S}} - \mathbf{1}) \circ (\boldsymbol{q}_{\mathcal{B}_{1}/\mathcal{S}} - \mathbf{1})$$

$$+ \frac{1}{2} \left(\boldsymbol{\omega}_{\mathcal{G}/\mathcal{E}}^{\mathcal{G}}\right)^{s} \circ \left(K_{\mathcal{G}} \star \left(\boldsymbol{\omega}_{\mathcal{G}/\mathcal{E}}^{\mathcal{G}}\right)^{s}\right) + p_{\mathcal{G}}(\boldsymbol{q}_{\mathcal{G}/\mathcal{E}} - \mathbf{1}) \circ (\boldsymbol{q}_{\mathcal{G}/\mathcal{E}} - \mathbf{1}) (40)$$

where • denotes the circle product given by [33,34]

$$\boldsymbol{a} \circ \boldsymbol{b} = a_{r} \cdot b_{r} + a_{d} \cdot b_{d} \in \mathbb{H}_{d}^{r} \tag{41}$$

where $a, b \in \mathbb{H}_d$. Note that V in Eq. (40) is a valid candidate Lyapunov function since

$$V\left(\boldsymbol{q}_{\mathcal{B}_{1}/\mathcal{S}}=\boldsymbol{1},\boldsymbol{\omega}_{\mathcal{B}_{1}/\mathcal{S}}^{\mathcal{B}_{1}}=\boldsymbol{0},\boldsymbol{q}_{\mathcal{G}/\mathcal{E}}=\boldsymbol{1},\boldsymbol{\omega}_{\mathcal{G}/\mathcal{E}}^{\mathcal{G}}=\boldsymbol{0}\right)=0\quad\text{and}$$

$$V\left(\boldsymbol{q}_{\mathcal{B}_{1}/\mathcal{S}},\boldsymbol{\omega}_{\mathcal{B}_{1}/\mathcal{S}}^{\mathcal{B}_{1}},\boldsymbol{q}_{\mathcal{G}/\mathcal{E}},\boldsymbol{\omega}_{\mathcal{G}/\mathcal{E}}^{\mathcal{G}}\right)>0\tag{42}$$

for all $(\boldsymbol{q}_{\mathcal{B}_1/\mathcal{S}}, \boldsymbol{\omega}_{\mathcal{B}_1/\mathcal{S}}^{\mathcal{B}_1}, \boldsymbol{q}_{\mathcal{G}/\mathcal{E}}, \boldsymbol{\omega}_{\mathcal{G}/\mathcal{E}}^{\mathcal{G}}) \in \mathbb{H}_d^u \times \mathbb{H}_d^v \times \mathbb{H}_d^u \times \mathbb{H}_d^v \setminus \{(\mathbf{1.0}, \mathbf{1.0})\}.$ It is straightforward to show that the time derivative of V in Eq. (40) is given by

From the assumption that the dynamics matrix $\Psi(\bar{x})_{1,N}$ can be allocated such that, $\Phi_1(\bar{x})$, $\Phi_N(\bar{x}) \in \mathcal{L}_{\infty}$, and letting $\alpha(q^0_{\mathcal{B}_1/\mathcal{S},r}) = \alpha(q^0_{\mathcal{G}/\mathcal{E},r}) = 1$, then implementing the control law proposed in Eq. (37) into Eq. (45), it follows that

$$\dot{V} = -k_{\mathcal{B}_{1}} \left(\boldsymbol{\omega}_{\mathcal{B}_{1}/\mathcal{S}}^{\mathcal{B}_{1}} \right)^{s} \circ \left(\boldsymbol{\omega}_{\mathcal{B}_{1}/\mathcal{S}}^{\mathcal{B}_{1}} \right)^{s} - k_{\mathcal{G}} \left(\boldsymbol{\omega}_{\mathcal{G}/\mathcal{E}}^{\mathcal{G}} \right)^{s} \circ \left(\boldsymbol{\omega}_{\mathcal{G}/\mathcal{E}}^{\mathcal{G}} \right)^{s} \le 0$$

$$(46)$$

for all $(q_{\mathcal{B}_1/\mathcal{S}}, \omega_{\mathcal{B}_1/\mathcal{S}}^{\mathcal{B}_1}, q_{\mathcal{G}/\mathcal{E}}, \omega_{\mathcal{G}/\mathcal{E}}^{\mathcal{G}}) \in \mathbb{H}_d^u \times \mathbb{H}_d^v \times \mathbb{H}_d^u \times \mathbb{H}_d^v \setminus \{(\mathbf{1.0}, \mathbf{1.0})\},$ guaranteeing that $q_{\mathcal{B}_1/\mathcal{S}}, \omega_{\mathcal{B}_1/\mathcal{S}}^{\mathcal{B}_1}, q_{\mathcal{G}/\mathcal{E}}, \omega_{\mathcal{G}/\mathcal{E}}^{\mathcal{G}}$ are uniformly bounded, i.e., $q_{\mathcal{B}_1/\mathcal{S}}, \omega_{\mathcal{B}_1/\mathcal{S}}^{\mathcal{B}_1}, q_{\mathcal{G}/\mathcal{E}}, \omega_{\mathcal{G}/\mathcal{E}}^{\mathcal{G}} \in \mathcal{L}_{\infty}$.

Before continuing the analysis further, we note that in the case when the dual quaternions $q_{\mathcal{B}_1/\mathcal{S}}$, $q_{\mathcal{G}/\mathcal{E}}$ switch sign due to the double cover of pose representation, i.e., when the relative rotations about the principle axes exceed a motion greater than $\pm 180^{\circ}$ (in an axis-angle sense), the Lyapunov candidate function in Eq. (40) becomes

$$V\left(\boldsymbol{q}_{\mathcal{B}_{1}/\mathcal{S}},\boldsymbol{\omega}_{\mathcal{B}_{1}/\mathcal{S}}^{\mathcal{B}_{1}},\boldsymbol{q}_{\mathcal{G}/\mathcal{E}},\boldsymbol{\omega}_{\mathcal{G}/\mathcal{E}}^{\mathcal{G}}\right)$$

$$=\frac{1}{2}\left(\boldsymbol{\omega}_{\mathcal{B}_{1}/\mathcal{S}}^{\mathcal{B}_{1}}\right)^{s} \circ \left(K_{\mathcal{B}_{1}} \star \left(\boldsymbol{\omega}_{\mathcal{B}_{1}/\mathcal{S}}^{\mathcal{B}_{1}}\right)^{s}\right) + p_{\mathcal{B}_{1}}(-\boldsymbol{q}_{\mathcal{B}_{1}/\mathcal{S}}-1) \circ (-\boldsymbol{q}_{\mathcal{B}_{1}/\mathcal{S}}-1)$$

$$+\frac{1}{2}\left(\boldsymbol{\omega}_{\mathcal{G}/\mathcal{E}}^{\mathcal{G}}\right)^{s} \circ \left(K_{\mathcal{G}} \star \left(\boldsymbol{\omega}_{\mathcal{G}/\mathcal{E}}^{\mathcal{G}}\right)^{s}\right) + p_{\mathcal{G}}(-\boldsymbol{q}_{\mathcal{G}/\mathcal{E}}-1) \circ (-\boldsymbol{q}_{\mathcal{G}/\mathcal{E}}-1)$$

$$(47)$$

where now the equilibrium point is $q_{\mathcal{G}/\mathcal{E}} = -1$, $\omega_{\mathcal{G}/\mathcal{E}}^{\mathcal{G}} = 0$, $q_{\mathcal{B}_1/\mathcal{S}} = -1$, and $\omega_{\mathcal{B}_1/\mathcal{S}}^{\mathcal{B}_1} = 0$ of the closed-loop system formed by Eqs. (32), (33), and (37). Note that Eq. (47) establishes a valid candidate Lyapunov function given that $V(q_{\mathcal{B}_1/\mathcal{S}} = -1, \omega_{\mathcal{B}_1/\mathcal{S}}^{\mathcal{B}_1} = 0, q_{\mathcal{G}/\mathcal{E}} = -1$, $\omega_{\mathcal{G}/\mathcal{E}}^{\mathcal{G}} = 0$) = 0, and $V(q_{\mathcal{B}_1/\mathcal{S}}, \omega_{\mathcal{B}_1/\mathcal{S}}^{\mathcal{B}_1}, q_{\mathcal{G}/\mathcal{E}}, \omega_{\mathcal{G}/\mathcal{E}}^{\mathcal{G}}) > 0$ for all $(q_{\mathcal{B}_1/\mathcal{S}}, q_{\mathcal{G}/\mathcal{E}}, \omega_{\mathcal{B}_1/\mathcal{S}}^{\mathcal{G}}, q_{\mathcal{G}/\mathcal{E}}, \omega_{\mathcal{G}/\mathcal{E}}^{\mathcal{G}}) > 0$ for all $(q_{\mathcal{B}_1/\mathcal{S}}, q_{\mathcal{G}/\mathcal{E}}, \omega_{\mathcal{B}_1/\mathcal{S}}^{\mathcal{G}}, q_{\mathcal{G}/\mathcal{E}}, \omega_{\mathcal{G}/\mathcal{E}}^{\mathcal{G}}) > 0$ for all $(q_{\mathcal{B}_1/\mathcal{S}}, q_{\mathcal{G}/\mathcal{E}}, \omega_{\mathcal{B}_1/\mathcal{S}}^{\mathcal{G}}, q_{\mathcal{G}/\mathcal{E}}, \omega_{\mathcal{B}_1/\mathcal{S}}^{\mathcal{G}}, q_{\mathcal{G}/\mathcal{E}}, \omega_{\mathcal{B}_1/\mathcal{S}}^{\mathcal{G}}, q_{\mathcal{G}/\mathcal{E}}, \omega_{\mathcal{B}_1/\mathcal{S}}^{\mathcal{G}}, q_{\mathcal{G}/\mathcal{E}}, \omega_{\mathcal{B}_1/\mathcal{S}}^{\mathcal{G}}, q_{\mathcal{G}/\mathcal{E}}, \omega_{\mathcal{B}_1/\mathcal{S}}^{\mathcal{G}}, q_{\mathcal{B}/\mathcal{E}}, \omega_{\mathcal{B}_1/\mathcal{S}}^{\mathcal{G}}, q_{\mathcal{B}/\mathcal{E}}, \omega_{\mathcal{B}_1/\mathcal{S}}^{\mathcal{G}}, q_{\mathcal{B}/\mathcal{E}}, \omega_{\mathcal{B}_1/\mathcal{S}}^{\mathcal{G}}, q_{\mathcal{B}/\mathcal{E}}, \omega_{\mathcal{B}_1/\mathcal{S}}^{\mathcal{G}}, q_{\mathcal{B}/\mathcal{E}}, \omega_{\mathcal{B}/\mathcal{B}}^{\mathcal{G}}, q_{\mathcal{B}/\mathcal{E}}, \omega_{\mathcal{B}/\mathcal{B}/\mathcal{B}}^{\mathcal{G}}, q_{\mathcal{B}/\mathcal{B}}, q_{\mathcal{B}/\mathcal{B}}, q_{\mathcal{B}/\mathcal{B}/\mathcal{B}}^{\mathcal{G}}, q_{\mathcal{B}/\mathcal{B}/\mathcal{B}}, q_{\mathcal{B}/\mathcal{B}/\mathcal{B}}^{\mathcal{G}}, q_{\mathcal{B}/\mathcal{B}/\mathcal{B}}^{\mathcal{G}}, q_{\mathcal{B}/\mathcal{B}/\mathcal{B}}^{\mathcal{G}}, q_{\mathcal{B}/\mathcal{B}/\mathcal{B}}^{\mathcal{B}}, q_{\mathcal{B}/\mathcal{B}/\mathcal{B}/\mathcal{B}}^{\mathcal{B}}, q_{\mathcal{B}/\mathcal{B}/\mathcal{B}}^{\mathcal{B}}, q_{\mathcal{B}/\mathcal{B}/\mathcal{B}}^{\mathcal{B}}, q_{\mathcal{B}/\mathcal{B}/\mathcal{B}}^{\mathcal{B}}, q_{\mathcal{B}/\mathcal{B}/\mathcal{B}}^{\mathcal{B}}, q_{\mathcal{B}/\mathcal{B}/\mathcal{B}}^{\mathcal{B}}, q_{\mathcal{B}/\mathcal{B}/\mathcal{B}/\mathcal{B}}^{\mathcal{B}}, q_{\mathcal{B}/\mathcal{B}/\mathcal{B}/\mathcal{B}}^{\mathcal{B}}, q_{\mathcal{B}/\mathcal{B}/\mathcal{B}/\mathcal{B}}^{\mathcal{B}}, q_{\mathcal{B}/\mathcal{B}/\mathcal{B}/\mathcal{B}}^{\mathcal{B}}, q_{\mathcal{B}/\mathcal{B}/\mathcal{B}/\mathcal{B}}^{\mathcal{B}}, q_{\mathcal{B}/\mathcal{B}/\mathcal{B}}^{\mathcal{B}}, q_{\mathcal{B}/\mathcal{B}/\mathcal{B}/\mathcal{B}^$

A similar analysis to that given in Eqs. (43) and (44) determines that the derivative of Eq. (47) results in

^{**}The \mathcal{L}_{∞} -norm of a function $u:[0,\infty)\to\mathbb{H}_d$ is defined as $\|u\|_{\infty}=\sup_{t\geq 0}\|u(t)\|$. Moreover, the function $u\in\mathcal{L}_{\infty}$ if and only if $\|u\|_{\infty}<\infty$.

$$\dot{V} = \begin{bmatrix} \left(\boldsymbol{\omega}_{\mathcal{B}_{1}/\mathcal{S}}^{\mathcal{B}_{1}}\right)^{s} \\ \left(\boldsymbol{\omega}_{\mathcal{G}/\mathcal{E}}^{\mathcal{G}}\right)^{s} \end{bmatrix}^{\mathsf{T}} \circ \begin{bmatrix} p_{\mathcal{B}_{1}}\boldsymbol{q}_{\mathcal{B}_{1}/\mathcal{S}}^{*}(\boldsymbol{q}_{\mathcal{B}_{1}/\mathcal{S}}+\boldsymbol{1})^{s} + K_{\mathcal{B}_{1}} \star \left(\boldsymbol{\Phi}_{1}(\bar{x}) + \boldsymbol{\Psi}_{1}(\bar{x}) \star \boldsymbol{u}_{\mathcal{B}_{1}} - \dot{\boldsymbol{\omega}}_{\mathcal{S}/\mathcal{I}}^{\mathcal{B}_{1}}\right)^{s} \\ p_{\mathcal{G}}\boldsymbol{q}_{\mathcal{G}/\mathcal{E}}^{*}(\boldsymbol{q}_{\mathcal{G}/\mathcal{E}}+\boldsymbol{1})^{s} + K_{\mathcal{G}} \star \left(\boldsymbol{q}_{\mathcal{G}/\mathcal{B}_{N}}^{*}(\boldsymbol{\Phi}_{N}(\bar{x}) + \boldsymbol{\Psi}_{N}(\bar{x}) \star \boldsymbol{u}_{\mathbf{J}_{1:N}})\boldsymbol{q}_{\mathcal{G}/\mathcal{B}_{N}} - \dot{\boldsymbol{\omega}}_{\mathcal{E}/\mathcal{I}}^{\mathcal{G}}\right)^{s} \end{bmatrix}$$

$$(48)$$

Note that the only difference between Eqs. (45) and (48) is in the dual quaternion terms, i.e., $q^*(q-1)^s$ and $q^*(q+1)^s$, hence implementing the control law proposed in Eq. (37) into Eq. (48) and noting that the hybrid logic function $\alpha(\cdot)$ will switch the dual quaternion signage accordingly yields the same expression as in Eq. (46) for all $(q_{\mathcal{B}_1/\mathcal{S}}, \omega_{\mathcal{B}_1/\mathcal{S}}^{\mathcal{B}_1}, q_{\mathcal{G}/\mathcal{E}}, \omega_{\mathcal{G}/\mathcal{E}}^{\mathcal{G}}) \in \mathbb{H}_d^u \times \mathbb{H}_d^u \times \mathbb{H}_d^u \times \mathbb{H}_d^v \setminus \{(-1.0, -1.0)\},$ guaranteeing again that $q_{\mathcal{B}_1/\mathcal{S}}, \omega_{\mathcal{B}_1/\mathcal{S}}^{\mathcal{B}_1}, q_{\mathcal{G}/\mathcal{E}}, \omega_{\mathcal{G}/\mathcal{E}}^{\mathcal{G}}, \omega_{\mathcal{G}/\mathcal{E}}^{\mathcal{G}}$ are uniformly bounded, i.e., $q_{\mathcal{B}_1/\mathcal{S}}, \omega_{\mathcal{B}_1/\mathcal{S}}^{\mathcal{B}_1}, q_{\mathcal{G}/\mathcal{E}}, \omega_{\mathcal{G}/\mathcal{E}}^{\mathcal{G}} \in \mathcal{L}_{\infty}$.

Now, since $V \geq 0$ and $V \leq 0$, in either case of the dual quaternion

Now, since $V \ge 0$ and $\dot{V} \le 0$, in either case of the dual quaternion sign, the limit, $\lim_{t\to\infty} V(t)$, exists and is finite. Integrating both sides of Eq. (46), one obtains

$$\lim_{t \to \infty} \int_0^t -\dot{V}(\tau) \, d\tau = \lim_{t \to \infty} \int_0^t \left(k_{\mathcal{B}_1} \left(\boldsymbol{\omega}_{\mathcal{B}_1/\mathcal{S}}^{\mathcal{B}_1}(\tau) \right)^{s} \, \boldsymbol{\circ} \left(\boldsymbol{\omega}_{\mathcal{B}_1/\mathcal{S}}^{\mathcal{B}_1}(\tau) \right)^{s} + k_{\mathcal{G}} \left(\boldsymbol{\omega}_{\mathcal{G}/\mathcal{E}}^{\mathcal{G}}(\tau) \right)^{s} \, \boldsymbol{\circ} \left(\boldsymbol{\omega}_{\mathcal{G}/\mathcal{E}}^{\mathcal{G}}(\tau) \right)^{s} \right) d\tau \le V(0) \quad (49)$$

Since $q_{\mathcal{B}_1/\mathcal{S}}$, $\omega_{\mathcal{B}_1/\mathcal{S}}^{\mathcal{B}_1}$, $q_{\mathcal{G}/\mathcal{E}}$, $\omega_{\mathcal{G}/\mathcal{E}}^{\mathcal{G}} \in \mathcal{L}_{\infty}$ and by assumption $q_{\mathcal{E}/\mathcal{I}}$, $\dot{\omega}_{\mathcal{E}/\mathcal{I}}^{\mathcal{E}}$, $\omega_{\mathcal{E}/\mathcal{I}}^{\mathcal{E}}$, $q_{\mathcal{S}/\mathcal{I}}$, $\dot{\omega}_{\mathcal{S}/\mathcal{I}}^{\mathcal{E}}$, $\omega_{\mathcal{S}/\mathcal{I}}^{\mathcal{S}}$, $\omega_{\mathcal{S}/\mathcal{I}}^{\mathcal{S}} \in \mathcal{L}_{\infty}$, then given Eq. (34), and that $\omega_{\mathcal{G}/\mathcal{E}}^{\mathcal{E}} = q_{\mathcal{G}/\mathcal{E}}\omega_{\mathcal{G}/\mathcal{E}}^{\mathcal{G}}q_{\mathcal{G}/\mathcal{E}}^*$ and $\omega_{\mathcal{B}_1/\mathcal{S}}^{\mathcal{S}} = q_{\mathcal{B}_1/\mathcal{S}}\omega_{\mathcal{B}_1/\mathcal{S}}^{\mathcal{B}_1}q_{\mathcal{B}_1/\mathcal{S}}^*$, then $\dot{\omega}_{\mathcal{S}/\mathcal{I}}^{\mathcal{B}_1}$, $\dot{\omega}_{\mathcal{E}/\mathcal{I}}^{\mathcal{G}} \in \mathcal{L}_{\infty}$.

Given that $\dot{q}_{\mathcal{G}/\mathcal{B}_N} = 0$ implies that $q_{\mathcal{G}/\mathcal{B}_N} \in \mathcal{L}_{\infty}$, then it follows from Eq. (37) that $u \in \mathcal{L}_{\infty}$, which, given Eq. (33), implies that $\dot{\omega}_{\mathcal{B}_1/\mathcal{S}}^{\mathcal{B}_1}$, $\dot{\omega}_{\mathcal{G}/\mathcal{E}}^{\mathcal{G}} \in \mathcal{L}_{\infty}$. Since the integral of \dot{V} is finite and exists then, according to Barbalat's lemma [35], it follows that $\omega_{\mathcal{B}_1/\mathcal{S}}^{\mathcal{B}_1}(t) \to \mathbf{0}$ and $\omega_{\mathcal{G}/\mathcal{E}}^{\mathcal{G}}(t) \to \mathbf{0}$ as $t \to \infty$.

Additionally, it can be similarly shown that $\dot{\omega}_{\mathcal{B}_{1}/\mathcal{S}}^{\mathcal{B}_{1}}(t) \to \mathbf{0}$ and $\dot{\omega}_{\mathcal{G}/\mathcal{E}}^{\mathcal{G}}(t) \to \mathbf{0}$ as $t \to \infty$. To see this, notice that the limit $\lim_{t \to \infty} \int_{0}^{t} (\dot{\omega}_{\mathcal{B}_{1}/\mathcal{S}}^{\mathcal{B}_{1}}(\tau) + \dot{\omega}_{\mathcal{G}/\mathcal{E}}^{\mathcal{G}}(\tau)) \, d\tau = -\dot{\omega}_{\mathcal{B}_{1}/\mathcal{S}}^{\mathcal{B}_{1}}(0) - \dot{\omega}_{\mathcal{G}/\mathcal{E}}^{\mathcal{G}}(0)$ exists and is finite. Since the time derivative of Eq. (33) is

$$\ddot{\boldsymbol{\omega}}_{\mathcal{B}_{1}/\mathcal{S}}^{\mathcal{B}_{1}} = -\mathbb{S}\left(K_{\mathcal{B}_{1}}^{-1}\right) \star \left(k_{\mathcal{B}_{1}}\dot{\boldsymbol{\omega}}_{\mathcal{B}_{1}/\mathcal{S}}^{\mathcal{B}_{1}} + p_{\mathcal{B}_{1}}\frac{d}{dt}\left[\operatorname{vec}\left(\boldsymbol{q}_{\mathcal{B}_{1}/\mathcal{S}}^{*}(\boldsymbol{q}_{\mathcal{B}_{1}/\mathcal{S}} - \mathbf{1})^{s}\right)^{s}\right]\right)$$

$$\ddot{\boldsymbol{\omega}}_{\mathcal{G}/\mathcal{E}}^{\mathcal{G}} = -\mathbb{S}\left(K_{\mathcal{G}}^{-1}\right) \star \left(k_{\mathcal{G}}\dot{\boldsymbol{\omega}}_{\mathcal{G}/\mathcal{E}}^{\mathcal{G}} + p_{\mathcal{G}}\frac{d}{dt}\left[\operatorname{vec}\left(\boldsymbol{q}_{\mathcal{G}/\mathcal{E}}^{*}(\boldsymbol{q}_{\mathcal{G}/\mathcal{E}} - \mathbf{1})^{s}\right)^{s}\right]\right)$$
(50)

and given that $q_{\mathcal{B}_1/\mathcal{S}}$, $\dot{q}_{\mathcal{B}_1/\mathcal{S}}$, $\dot{\omega}_{\mathcal{B}_1/\mathcal{S}}^{\mathcal{B}_1}$, $q_{\mathcal{G}/\mathcal{E}}$, $\dot{q}_{\mathcal{G}/\mathcal{E}}$, $\dot{\omega}_{\mathcal{G}/\mathcal{E}}^{\mathcal{G}}$ $\in \mathcal{L}_{\infty}$, it follows that $\ddot{\omega}_{\mathcal{B}_1/\mathcal{S}}^{\mathcal{B}_1}$, $\ddot{\omega}_{\mathcal{G}/\mathcal{E}}^{\mathcal{G}}$ $\in \mathcal{L}_{\infty}$. Hence, by Barbalat's lemma, $\dot{\omega}_{\mathcal{B}_1/\mathcal{S}}^{\mathcal{B}_1}$, $t \to 0$ and $\dot{\omega}_{\mathcal{G}/\mathcal{E}}^{\mathcal{G}}(t) \to 0$ as $t \to \infty$. Then calculating the limit as $t \to \infty$ of both sides of Eq. (33) with the control law given in Eq. (37) results in $-p_{\mathcal{B}_1} \text{vec}(q_{\mathcal{B}_1/\mathcal{S}}^*(t)(q_{\mathcal{B}_1/\mathcal{S}}(t)-1)^s)^s \to 0$, and $-p_{\mathcal{G}} \text{vec}(q_{\mathcal{G}/\mathcal{E}}^*(t)(q_{\mathcal{G}/\mathcal{E}}(t)-1)^s)^s \to 0$, as $t \to \infty$, which as shown in [22], is equivalent to $q_{\mathcal{B}_1/\mathcal{S}}(t) \to \pm 1$, and $q_{\mathcal{G}/\mathcal{E}}(t) \to \pm 1$.

Remark 1: Theorem 1 states that $q_{\mathcal{B}_1/\mathcal{S}}$ and $q_{\mathcal{G}/\mathcal{E}}$ converge to either ± 1 . Note that $q_{\mathcal{B}_1/\mathcal{S}} = 1$ and $q_{\mathcal{B}_1/\mathcal{S}} = -1$ and $q_{\mathcal{G}/\mathcal{E}} = 1$ and $q_{\mathcal{G}/\mathcal{E}} = -1$ represent the same spacecraft base and end-effector poses,

Remark 2: Despite the fact that Remark 1 implies that the proposed control in Eq. (37) avoids potential unwinding during controller execution, a hysteresis half-width δ is necessary to establish robustness to noise-induced chattering, which may occur in the existence of an arbitrarily small piecewise-constant noise signal that, for initial conditions arbitrarily close to the discontinuity of $q_r^0 = 0$, keeps the state near the discontinuity, for all time [27]. Thus, global asymptotic stability is guaranteed, although at the cost of a small region in the state space where the hybrid control law pulls the rigid body in the direction of longer rotation, determined from δ in the inequality in Eq. (39). Hence, the desired direction of rotation changes only when there is a significant benefit to switching, where "significant" is precisely defined by δ , which is selected to be commensurate with the anticipated noise magnitude, as represented in Fig. 2.

Remark 3: If the reference poses are constant in time, i.e., $\boldsymbol{\omega}_{\mathcal{E}/\mathcal{I}}^{\mathcal{E}} = \boldsymbol{\omega}_{\mathcal{S}/\mathcal{I}}^{\mathcal{E}} = \mathbf{0}$, then the SMRS pose-tracking controller suggested in Eq. (37) becomes a pose-stabilization controller.

IV. Actuator Allocation for Control of Multibody Systems

To simultaneously control the spacecraft base and the end effector of an SRMS, the collection of control wrenches u in Eq. (20) must be allocated throughout the maneuver. In Sec. III, we proved the global asymptotic stability of the proposed control law shown in Eq. (37), which necessitates a few key (strong) assumptions related to allocation. Specifically, although designing bounded reference trajectories is a feasible, although nontrivial task, designing reference trajectories such that, if exactly tracked by SMRSs, the matrix $\Psi_{1,N}(\bar{x})$ in Eq. (37) would remain well-conditioned and $\Phi_1(\bar{x})$, $\Phi_N(\bar{x}) \in \mathcal{L}_{\infty}$ is insufficient to guarantee boundedness of the control, as system singularities may occur during transients. Hence, in Secs. IV.A and IV.B, we detail an allocation policy that can guarantee that $\Psi_{1,N}(\bar{x})$ remains wellconditioned and $\Phi_1(\bar{x}), \Phi_N(\bar{x}) \in \mathcal{L}_{\infty}$ in Eq. (37) when void of system singularities, and can effectively mitigate ill-conditioned dynamics scenarios that lead to unbounded control, with minimum error during pose tracking.

A. Dynamic System Singularities

Consider the mapping from dual actuation wrenches to real-valued actuation wrenches given by

$$\bar{\mu}_j = \Pi_j \circledast \boldsymbol{u}_j \tag{51}$$

where the collection of real-valued actuation wrenches is given by

$$\bar{\mu} = \left[\left(\tilde{W}_{B_{1},act}^{\mathcal{B}_{1}}(O_{\mathcal{B}_{1}}) \right)^{\mathsf{T}} \left(\tilde{W}_{J_{i},act}^{\mathcal{J}_{i}}(O_{\mathcal{J}_{i}}) \right)^{\mathsf{T}} \cdots \left(\tilde{W}_{J_{N-1},act}^{\mathcal{J}_{N-1}}(O_{\mathcal{J}_{N-1}}) \right)^{\mathsf{T}} \right]^{\mathsf{T}} \\
\in \mathbb{R}^{(6+D)} \tag{52}$$

Denoting η as the right-hand side of the control law in Eq. (37),

$$\eta = \begin{bmatrix} -\Phi_{1}(\bar{x}) + \dot{\boldsymbol{\omega}}_{S/\mathcal{I}}^{\mathcal{B}_{1}} + S\left(K_{\mathcal{B}_{1}}^{-1}\right) \star \left[-k_{\mathcal{B}_{1}}\boldsymbol{\omega}_{\mathcal{B}_{1}/S}^{\mathcal{B}_{1}} - p_{\mathcal{B}_{1}}\operatorname{vec}\left(\boldsymbol{q}_{\mathcal{B}_{1}/S}^{*}\left(\boldsymbol{q}_{\mathcal{B}_{1}/S} - \alpha\left(q_{\mathcal{B}_{1}/S,r}^{0}\right)\mathbf{1}\right)^{s}\right)^{s}\right] \\ -\Phi_{N}(\bar{x}) + \boldsymbol{q}_{\mathcal{G}/\mathcal{B}_{N}}\left(\dot{\boldsymbol{\omega}}_{\mathcal{E}/\mathcal{I}}^{\mathcal{G}} + S\left(K_{\mathcal{G}}^{-1}\right) \star \left[-k_{\mathcal{G}}\boldsymbol{\omega}_{\mathcal{G}/\mathcal{E}}^{\mathcal{G}} - p_{\mathcal{G}}\operatorname{vec}\left(\boldsymbol{q}_{\mathcal{G}/\mathcal{E}}^{*}\left(\boldsymbol{q}_{\mathcal{G}/\mathcal{E}} - \alpha\left(q_{\mathcal{G}/\mathcal{E},r}^{0}\right)\mathbf{1}\right)^{s}\right)^{s}\right]\right)\boldsymbol{q}_{\mathcal{G}/\mathcal{B}_{N}}^{*} \end{bmatrix}$$

$$(53)$$

respectively. Such double cover representation of the pose can lead to unwinding [29]. However, since the control law in Eq. (37) implements the dynamic memory state function α , the control is guaranteed to properly regulate the poles in the event of dual quaternion sign switching, thus avoiding the unwinding phenomenon altogether.

then we can express the real-valued equivalent expression of the control law given in Eq. (37) for nonredundant and redundant space-craft systems as

$$\Psi_{1,N}(\bar{x})\Xi \circledast \boldsymbol{u} = \bar{\Psi}_{1,N}(\bar{x})\bar{\mu} = \bar{\eta}$$
 (54)

where $\Xi = \text{blkdiag}(\Pi_{B_1}, \Pi_1, \dots, \Pi_j, \dots, \Pi_{N-1})$, and given a slightly abuse the notation such that $\bar{\cdot}$ signifies the reduction of dimensionality of each row of η . In order for realizable real-valued, bounded control, $\bar{\mu}$, to exist in Eq. (54), the matrix $\bar{\Psi}_{1,N}(\bar{x})$ must be well-conditioned. Thus, we define a *singularity* for an SRMS as the states, \bar{x}_s , such that rank $(\bar{\Psi}_{1,N}(\bar{x}_s)) < M = 6 + D$.

B. Mitigating Singular Neighborhoods via Optimal Damped Least Squares

One solution to mitigate singular neighborhoods where the matrix $\bar{\Psi}_{1,N}(x)$ becomes ill-conditioned and the control inputs become unbounded is to solve the following minimization problem [36–38]:

$$\begin{aligned} &\min & \|\bar{\ell}\|_2^2 \\ &\text{subject to } \bar{\eta} = \bar{\Psi}_{1,N}(\bar{x})\bar{\mu} + \bar{\ell}, \\ &\|\bar{\mu}\|_2^2 \leq \gamma \end{aligned} \tag{55}$$

where $\bar{\ell}$ denotes the error incurred in tracking, and a control input vector $\bar{\mu}$ is only feasible if its norm is less than or equal to a maximum permissible value γ . Using the first-order necessary conditions, the solution to Eq. (55) is given as

$$\bar{\mu}_{\lambda}^* = \bar{\Psi}_{1,\mathrm{N}}^{\mathsf{T}}(\bar{x}) \Big(\bar{\Psi}_{1,\mathrm{N}}(\bar{x}) \bar{\Psi}_{1,\mathrm{N}}^{\mathsf{T}}(\bar{x}) + \lambda I \Big)^{-1} \bar{\eta} \tag{56}$$

where $\lambda \ge 0$ and $\lambda(\|\bar{\mu}_{\lambda}^*\|^2 - \gamma^2) = 0$. Thus, the solution to Eq. (55) ensures the following:

- a) If $\lambda=0$ and $\|\bar{\mu}_0^*\| \leq \gamma$, then $\bar{\mu}_0^*=\bar{\mu}_0^+=\bar{\Psi}_{1,N}^+(\bar{x})\bar{\eta}$, i.e., the pseudo-inverse, is the exact solution.
- b) If $\lambda>0$ and $\|\bar{\mu}_\lambda^*\|=\gamma$, then $\bar{\mu}_\lambda^*$ in Eq. (56) is the damped least-squares solution.

Thus, whenever the pseudo-inverse solution yields a control norm less than or equal to the allowable norm γ , the solution to Eq. (55) is equal to the pseudo-inverse and the optimal damping factor is $\lambda = 0$.

The solution to Eq. (55) is related to solving the nonlinear equation in λ in order to compute the optimal damping factor

$$\phi(\lambda) - \gamma = \left\| \bar{\Psi}_{1,N}^{\mathsf{T}}(\bar{x}) \left(\bar{\Psi}_{1,N}(\bar{x}) \bar{\Psi}_{1,N}^{\mathsf{T}}(\bar{x}) + \lambda I \right)^{-1} \bar{\eta} \right\| - \gamma = 0 \quad (57)$$

where whenever $\phi(0) > \gamma$, then the pseudo-inverse solution is infeasible. Using the singular value decomposition (SVD) of the matrix $\bar{\Psi}_{1,N}(\bar{x})$, i.e., SVD $(\bar{\Psi}_{1,N}(\bar{x})) = UDV^{\mathsf{T}}$, it follows

$$\phi(\lambda) = \sqrt{\sum_{i=1}^{M} \frac{\sigma_i^2 \nu_i^2}{(\sigma_i^2 + \lambda)^2}}$$
 (58)

given that $U^{\mathsf{T}}\bar{\eta} = [\nu_i, \dots, \nu_M]^{\mathsf{T}}$. Differentiating $\phi(\lambda)$ from Eq. (58) with respect to λ , we obtain

$$\phi'(\lambda) = -\frac{1}{\|\bar{\mu}_{\lambda}^*\|} \sum_{i=1}^{M} \frac{\sigma_i^2 \nu_i^2}{(\sigma_i^2 + \lambda)^3}$$
 (59)

where we see that $\phi'(\lambda) < 0$ for $\lambda \ge 0$. As shown in [37], $\phi''(\lambda) > 0$ for $\lambda \ge 0$; thus, $\phi(\lambda)$ is a continuous, strictly decreasing function for $\lambda \in [0, +\infty)$ and $\phi(\lambda)$ approaches $-\gamma$ as λ tends to infinity. Hence, if $\phi(0) > \gamma$, i.e., the norm of the pseudo-inverse solution is greater than γ , it follows that there is a unique $\lambda^* > 0$ such that $\phi(\lambda^*) = \gamma$. Finally, the damping factor can be determined by applying Newton's method to the iteration [37]

$$\lambda_{k+1} = \lambda_k - \left\lceil \frac{\phi(\lambda_k)}{\gamma} \right\rceil \left\lceil \frac{\phi(\lambda_k) - \gamma}{\phi'(\lambda_k)} \right\rceil \tag{60}$$

1. Selective Control Dampening via Numerical Filtering

Note that the solution to the minimization in Eq. (55) is inherently conservative in that all of the control inputs are uniformly penalized by the same damping factor λ , even though the system singularity may only be attributed to a single singular direction (in an SVD sense). Hence, given a singularity in the dynamics matrix $\bar{\Psi}_{1,N}(\bar{x})$ when implementing the allocation given in Eq. (56), it may result unnecessarily in a uniform pose-tracking error for both the spacecraft base and end effector(s).

To this end, and without loss of generality, the damped least-squares solution in Eq. (56) can be augmented for *selective* damping of the control input by numerically filtering the control input that corresponds to the smallest singular value σ_M . Specifically, we augment the optimal damped least-squares allocation solution in Eq. (56) such that [39,40]

$$\bar{\mu}_{\lambda,\beta}^* = \bar{\Psi}_{1,N}^{\mathsf{T}}(\bar{x}) \Big(\bar{\Psi}_{1,N}(\bar{x}) \bar{\Psi}_{1,N}^{\mathsf{T}}(\bar{x}) + \lambda I + \beta \bar{u}_{\mathsf{M}} \bar{u}_{\mathsf{M}}^{\mathsf{T}} \Big)^{-1} \bar{\eta}$$
 (61)

where $\bar{u}_{\rm M}$ is the output singular vector associated with singular value $\sigma_{\rm M}$ of the matrix $\bar{\Psi}_{1,\rm N}(\bar{x})$ and β is given by [41]

$$\beta = \begin{cases} 0, & \text{when } \|\bar{\mu}\|_{2}^{2} \le \gamma \\ \left(1 - \left(\frac{\sigma_{M}}{\Delta}\right)^{2}\right) \beta_{\text{max}}, & \text{otherwise} \end{cases}$$
 (62)

where β_{max} sets the maximum value of the β damping factor and Δ defines the size of the singular region. Note that, after assigning β_{max} and Δ , the optimal control damping factor λ is still computed using Eqs. (58–60), given the updated selective damped least-squares solution given in Eq. (61).

The advantage of using the numerical filtering technique outlined in Eq. (61) is clear when we look at the norm of the solutions. Specifically, it is clear that when no dampening is required (i.e., when $\|\bar{\mu}\|_2^2 \leq \gamma$), then the pseudo-inverse solution norm given by

$$\|\bar{\mu}_0^*\| = \|\bar{\Psi}_{1,N}^+(\bar{x})\bar{\eta}\| = \sqrt{\sum_{i=1}^M \frac{\nu_i^2}{\sigma_i^2}}$$
 (63)

yields the lowest possible value.

If the minimization in Eq. (55) does require dampening, and we naïvely uniformly dampen the solution given the allocation policy in Eq. (56), then the solution norm is given by

$$\|\bar{\mu}_{\lambda}^*\| = \sqrt{\sum_{i=1}^M \frac{\sigma_i^2 \nu_i^2}{(\sigma_i^2 + \lambda)^2}}$$
 (64)

However, if we implement the numerically filtered damped least-squares solution given in Eq. (61), the solution norm is now given as

$$\|\bar{\mu}_{\lambda,\beta}^*\| = \sqrt{\sum_{i=1}^{M-1} \frac{\sigma_i^2 \nu_i^2}{(\sigma_i^2 + \lambda)^2}} + \sqrt{\frac{\sigma_M^2 \nu_M^2}{(\sigma_M^2 + \lambda + \beta)^2}}$$
(65)

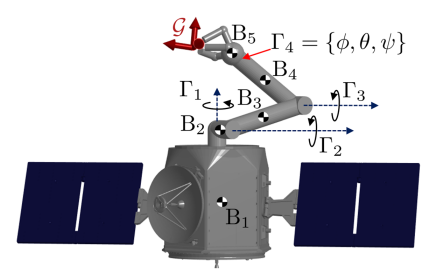


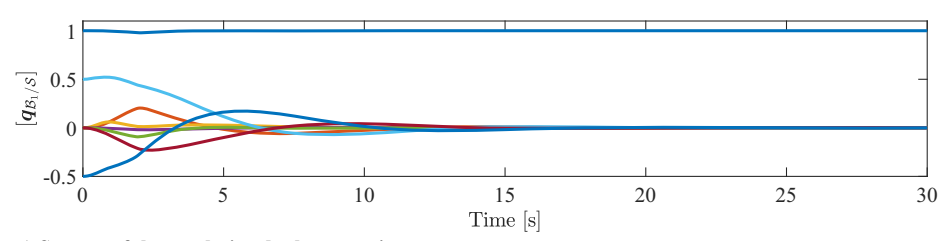
Fig. 3 Nonredundant multibody RRRS SRMS with generalized coordinates Γ and end-effector frame \mathcal{G} .

Table 1 RRRS SMRS parameters

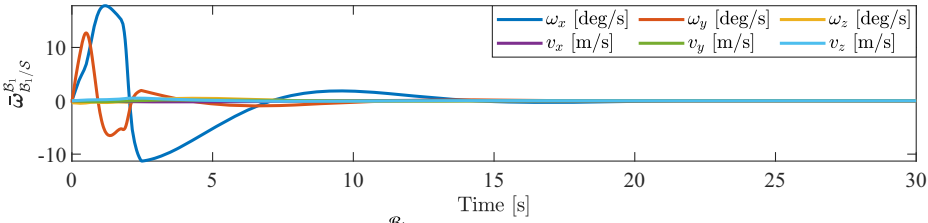
Body	Mass, kg	Inertia $[I_{xx}, I_{yy}, I_{zz}]$, kg/m ²		
B_1	120	[14, 14, 14]		
B_2	10	[0.5, 2, 2]		
B_3	10	[0.5,2,2]		
B_4	10	[0.5,2,2]		
B_5	10	[1, 1, 1]		
Index i, j	$\bar{r}_{\mathcal{O}_{\mathcal{I}_j}/\mathcal{O}_{\mathcal{B}_i}}^{\mathcal{B}_i} = [r_x, r_y, r_z], [m]$	$\bar{r}_{\mathrm{O}_{\mathcal{B}_{i+1}}/\mathrm{O}_{\mathcal{I}_j}}^{\mathcal{J}_j} = [r_x, r_y, r_z], [\mathrm{m}]$		
1	[0, 0, 1.65]	[0, 0, 0.25]		
2	[0, 0.05, 0]	[-1.1, 0, 0.4]		
3	[-1.1, 0, -0.05]	[-1.1,0,-0.2]		
4	[-1.1, 0, 0]	[0, 0, 0.1]		
End-effector translational offset				
$ar{r}_{\mathrm{O}_{\mathcal{G}}}^{\mathcal{B}_{5}}$	[0, 0, 0.9]			

where it is now evident that the last term on the right-hand side of Eq. (65) is the term that induces the largest contribution to the control input norm solution. Without the filter dampening gain β , the damping factor λ is forced to increase uniformly, as shown in Eq. (64), unnecessarily damping the well-behaved components in the summation term and resulting in unnecessary tracking error. Hence β dampens the solution along the singular direction associated with the smallest singular value of the control inputs while simultaneously diminishing the amount of necessary dampening from λ to well-behaved solution regions to satisfy the minimization in Eq. (55).

In Sec. V, we implement the selective damped least-squares solution in Eq. (61) such that we guarantee the allocation of the dynamics matrix $\Psi_{1,N}(\bar{x})$ and that $\Phi_1(\bar{x})$, $\Phi_N(\bar{x}) \in \mathcal{L}_{\infty}$ while executing the control law given in Eq. (37) when $\|\bar{\mu}\|_2^2 \leq \gamma$ from the minimization in Eq. (55), and when dampening is required, we determine the minimum deviation from the desired reference trajectories via numerical filtering.

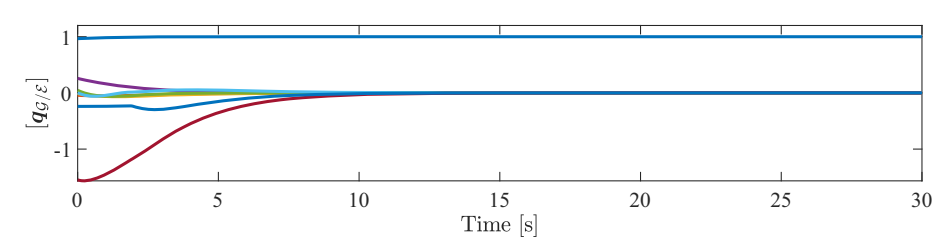


a) Spacecraft base relative dual quaternion $q_{\mathcal{B}_1/\mathcal{S}}$

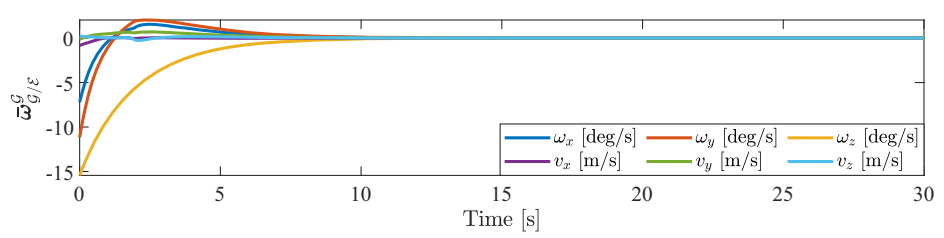


b) Spacecraft base relative dual velocity $\omega_{\mathcal{B}_1/\mathcal{S}}^{\mathcal{B}_1}$

Fig. 4 Positive pole regulation, i.e., $q_{\mathcal{B}_1/\mathcal{S}} \to 1$ and $\omega_{\mathcal{B}_1/\mathcal{S}}^{\mathcal{B}_1} \to 0$ as $t \to \infty$, during pose tracking.

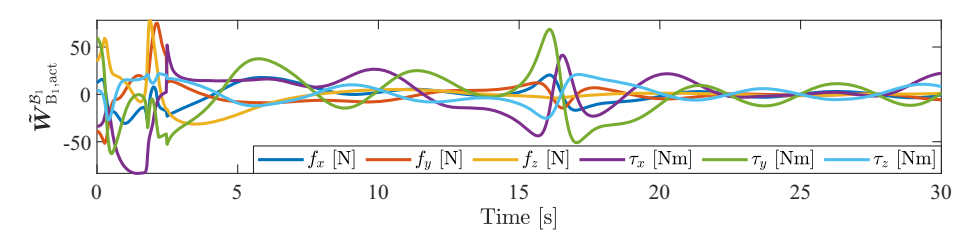


a) Manipulator end-effector relative dual quaternion $q_{G/\mathcal{E}}$

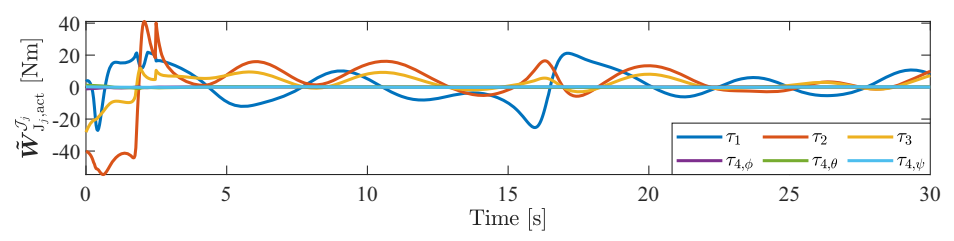


b) Manipulator end-effector relative dual velocity $\omega_{\mathcal{G}/\mathcal{E}}^{\mathcal{G}}$

Fig. 5 Positive pole regulation, i.e., $q_{\mathcal{G}/\mathcal{E}} \to 1$ and $\omega_{\mathcal{G}/\mathcal{E}}^{\mathcal{G}} \to 0$ as $t \to \infty$, during pose tracking.

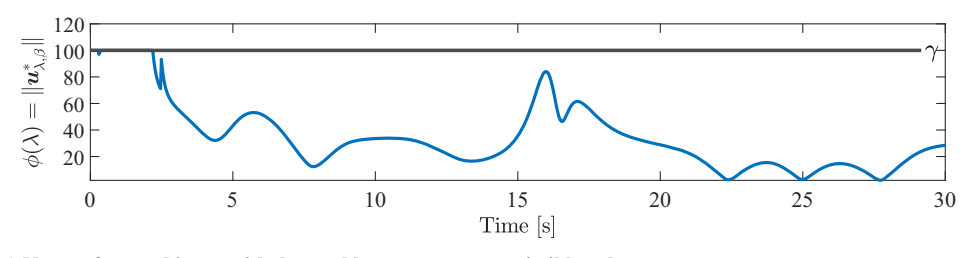


a) Generalized control forces and torques applied to spacecraft base

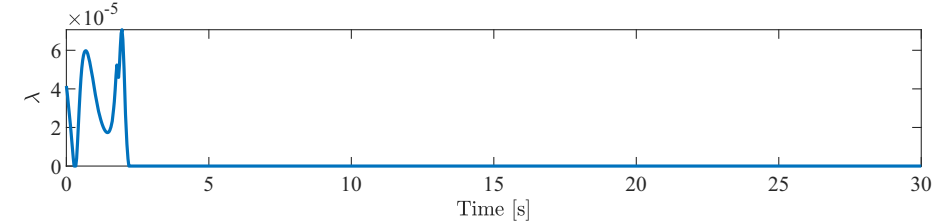


b) Control torques applied to the manipulator

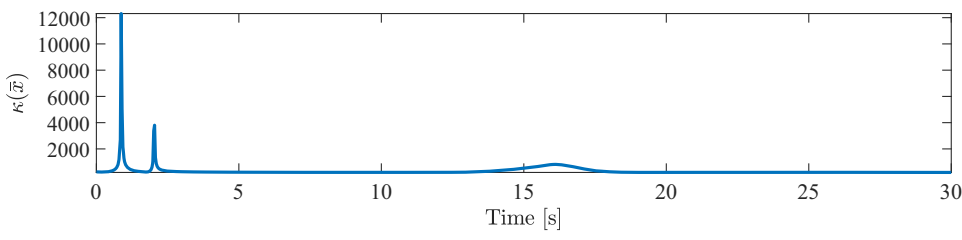
Fig. 6 Reduced real-value dual wrenches applied to the RRRS SMRS during pose tracking.



a) Norm of control input with damped least-squares permissible value γ



b) Optimal control dampening factor λ



c) Condition number $\kappa(\bar{x})$, of the dynamics matrix $\bar{\Psi}_{1,N}(\bar{x})$

Fig. 7 Optimal damped least-squares actuator allocation during RRRS SMRS pose tracking.

V. Numerical Simulations

In this section, we illustrate the global asymptotic stability of the proposed dual quaternion control law given in Eq. (37) and selective damped least-squares actuator allocation policy Eq. (61) on a non-redundant RRRS^{††} SRMS, modeled from NASA's Transition Exoplanet Survey Satellite [42], as shown in Fig. 3.

The parameters of the RRRS SMRS are given in Table 1. We denote $\kappa(\bar{x})$ as the condition number of the matrix $\bar{\Psi}_{1,N}(\bar{x})$ (here N=5 bodies), such that $\kappa(\bar{x})$ is a measure of the RRRS SMRS singularities. A small condition number of $\bar{\Psi}_{1,N}(\bar{x})$ implies that $\bar{\Psi}_{1,N}(\bar{x})$ is well-conditioned and void of singularities.

For all of the numerical simulations given in Secs. V.A and V.B, we choose to implement the controller in Eq. (37), with the following gains $K_{\mathcal{B}_1}=K_{\mathcal{G}}=I$, $p_{\mathcal{B}_1}=k_{\mathcal{B}_1}=0.5$, $p_{\mathcal{G}}=1$, and $k_{\mathcal{G}}=1.5$, given hysteresis half-half $\delta=0.5$ for the inequality in Eq. (39), and let $\Delta=0.5$, $\beta_{\max}=10$, and $\gamma=100$ in the numerically filtered selective damped least-squares allocator given in Eqs. (61) and (62) respectively.

A. Global Simultaneous SMRS Spacecraft Base and End-Effector Pose Tracking

In this section, we illustrate pose tracking with both positive and negative dual quaternion pole regularization to show the global asymptotic stable behavior of the proposed control in Eq. (37). In both cases, reference trajectories were designed for tracking such that

^{††}R: revolute; S, spherical.

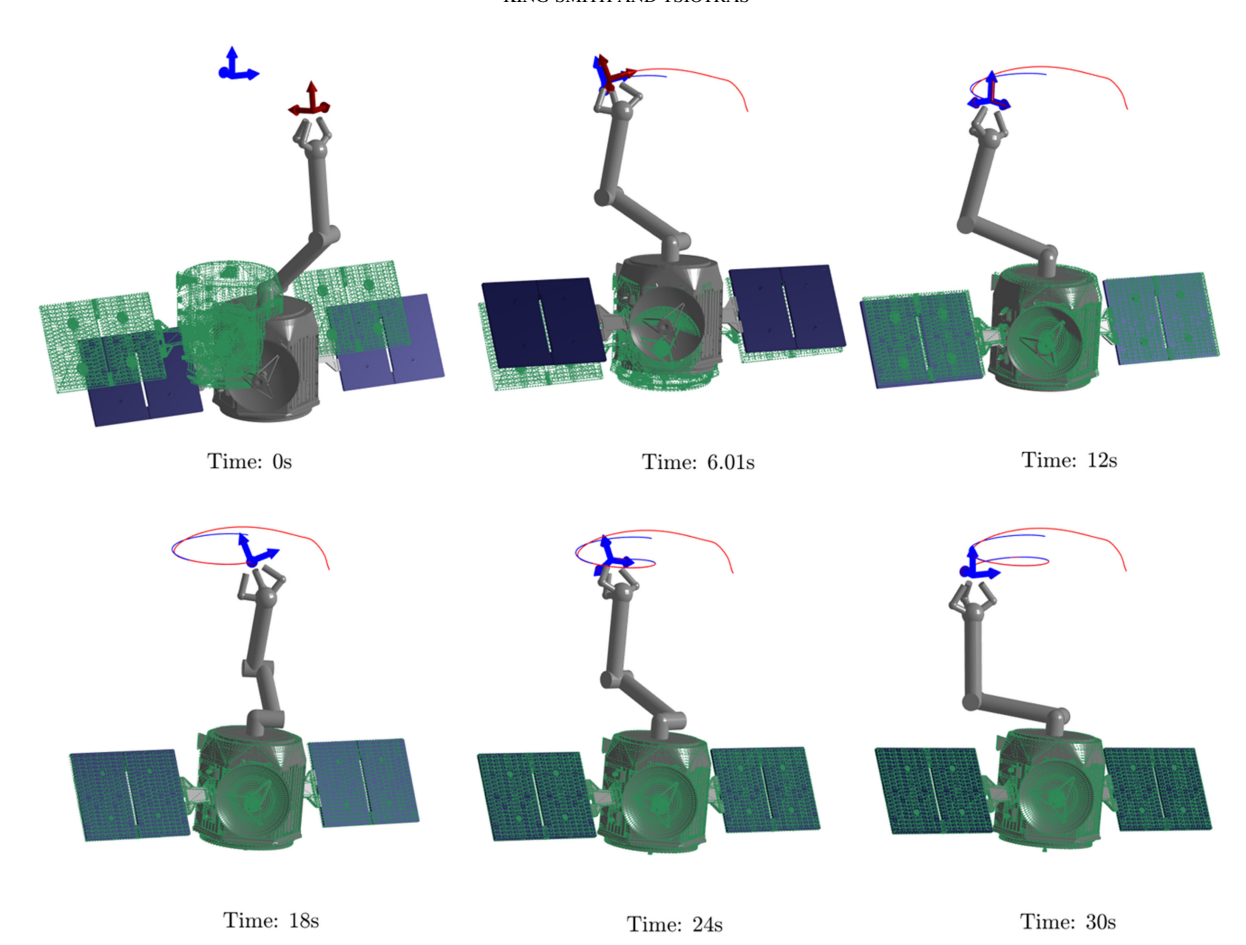


Fig. 8 Animation of the tracking sequence of the SMRS-base and manipulator end effector. The end-effector frame $\mathcal G$ tracks reference frame $\mathcal E$ and the spacecraft base tracks the green wire mesh ($\mathcal S$ frame).

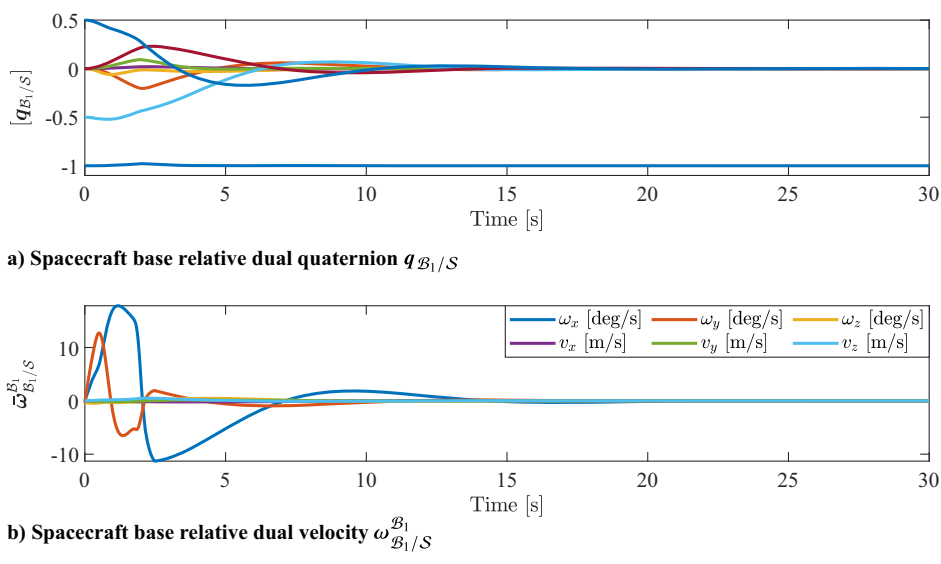


Fig. 9 Negative pole regulation, i.e., $q_{\mathcal{B}_1/\mathcal{S}} \to -1$ and $\omega_{\mathcal{B}_1/\mathcal{S}}^{\mathcal{B}_1} \to 0$ as $t \to \infty$, during pose tracking.

the combined motion of the reference trajectories remained within the reachable workspace of the RRRS SMRS given in Fig. 3.

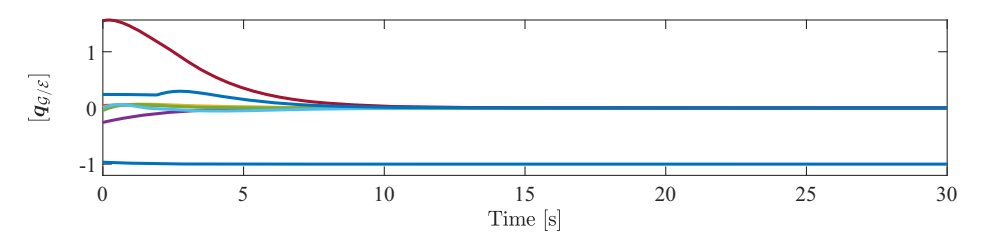
1. Positive Pole Regularization

Figures 4 and 5 illustrate the simultaneous asymptotic pose tracking achieved by the SMRS spacecraft base and end effector of the manipulator, respectively.

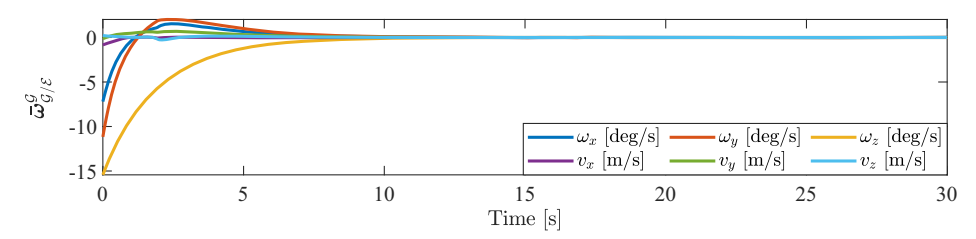
Figure 6 shows the real-valued generalized forces and torques applied to the spacecraft base and manipulator of the system

throughout the tracking maneuver. Note that the selective damped least-squares allocation necessitated tracking errors during the first 0 to 3.5 s of the maneuver, resulting in a nonzero value for λ , as shown in Fig. 7b, and dampening of the numerically filtered control $\boldsymbol{u}_{\lambda,\beta}^*$ to the permissible value γ , as shown in Fig. 7a, after which no dampening is required, allowing for pose tracking, as shown in Figs. 4 and 5.

Additionally, we see that the dampening of the control that occurs in Fig. 7 allows the allocation technique to mitigate a large condition

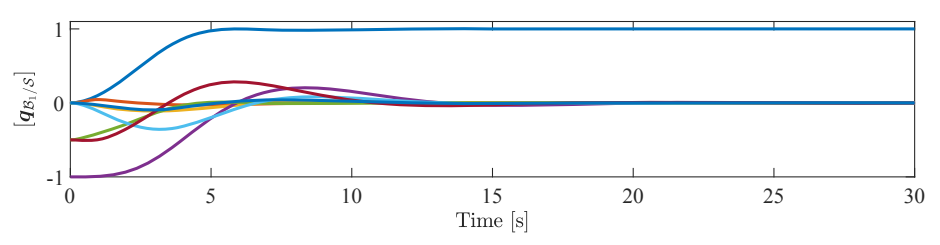


a) Manipulator end-effector relative dual quaternion $q_{\mathcal{G}/\mathcal{E}}$

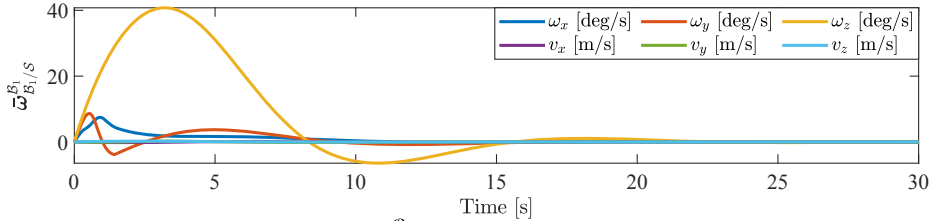


b) Manipulator end-effector relative dual velocity $\omega_{\mathcal{G}/\mathcal{E}}^{\mathcal{G}}$

Fig. 10 Negative pole regulation, i.e., $q_{\mathcal{G}/\mathcal{E}} \to -1$ and $\omega_{\mathcal{G}/\mathcal{E}}^{\mathcal{G}} \to 0$ as $t \to \infty$, during pose tracking.

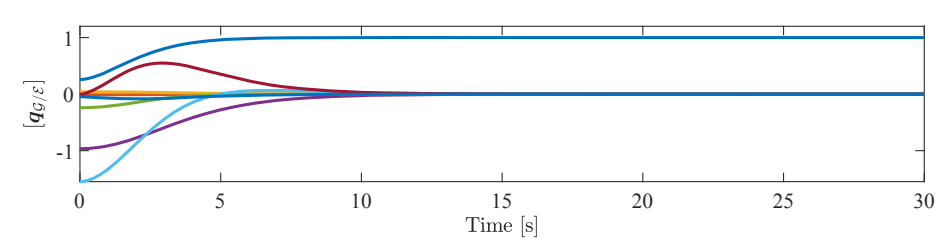


a) Spacecraft base relative dual quaternion $q_{\mathcal{B}_1/\mathcal{S}}$

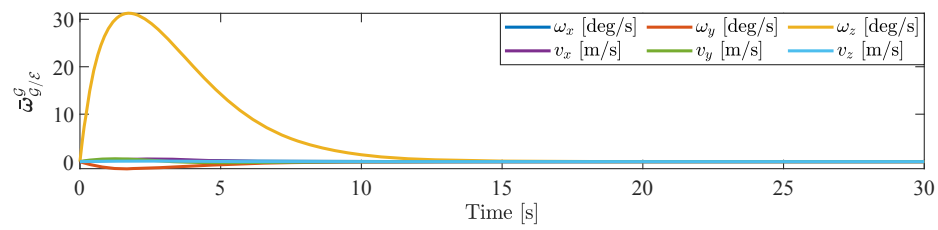


b) Spacecraft base relative dual velocity $\omega_{\mathcal{B}_1/\mathcal{S}}^{\mathcal{B}_1}$

Fig. 11 Chatter-free positive pole regulation, i.e., $q_{\mathcal{B}_1/\mathcal{S}} \to 1$ and $\omega_{\mathcal{B}_1/\mathcal{S}}^{\mathcal{B}_1} \to 0$ as $t \to \infty$, during pose stabilization with noisy feedback.



a) Manipulator end-effector relative dual quaternion $q_{\mathcal{G}/\mathcal{E}}$



b) Manipulator end-effector relative dual velocity $\omega_{\mathcal{G}/\mathcal{E}}^{\mathcal{G}}$

Fig. 12 Chatter-free positive pole regulation, i.e., $q_{\mathcal{G}/\mathcal{E}} \to 1$ and $\omega_{\mathcal{G}/\mathcal{E}}^{\mathcal{G}} \to 0$ as $t \to \infty$, during pose stabilization with noisy feedback.

number of the dynamics matrix $\bar{\Psi}_{1,N}(\bar{x})$, shown in Fig. 7c, at the beginning of the maneuver.

Finally, snapshots of an animation visualization of the entire tracking maneuver are shown in Fig. 8, where the complete animation can be found online at https://www.youtube.com/watch?v=Y8Ct8N_TnWY.

2. Negative Pole Regularization

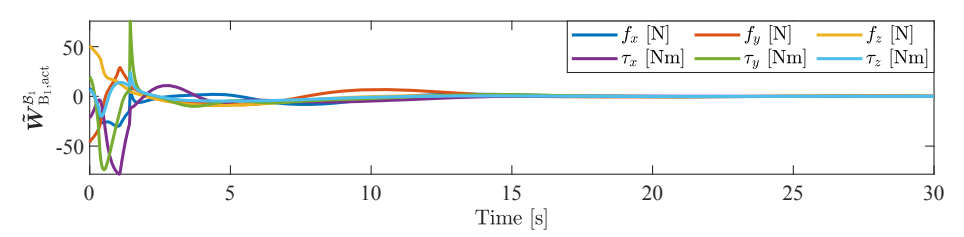
We adjust the reference trajectories for frames \mathcal{E} and \mathcal{S} to illustrate pose tracking with negative pole regularization, by simply adding 2π to the attitude references about the body-fixed z axis of each reference frame such that we achieve an identical maneuver as during positive pole regularization, but it now necessitates negative pole regularization, as shown in Figs. 9 and 10. Note that because the reference trajectories are only augmented about a single axis by 2π , the tracking

maneuver results in identical dual control wrenches, allocation, and animation plots as shown in Figs. 6–8, respectively.

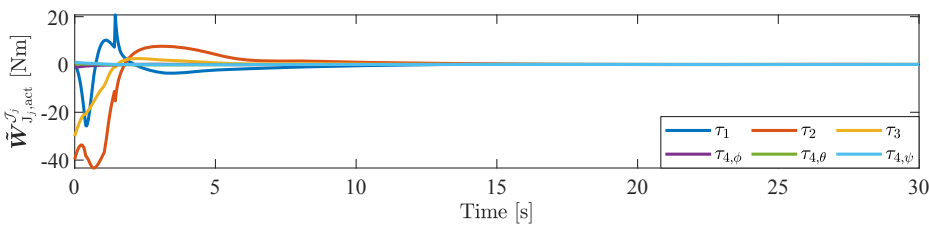
B. Pose Stabilization from Dual Quaternion Discontinuity $q_{\rm r}^0=0$

In addition to the pose tracking shown in Sec. V.A, we demonstrate pose stabilization starting from a configuration where the spacecraft base of the RRRS SMRS begins on the discontinuous boundary of $q_{B_1/S}^0 = 0$ such that we can illustrate the unwinding- and chatter-free nature of the proposed control in Eq. (37), as noted in Remarks 1–3. We additionally inject zero-mean white Gaussian noise into the relative dual quaternions, $\mathbf{q}_{B_1/S}$, $\mathbf{q}_{G/\mathcal{E}}$, to simulate the presence of noisy feedback and illustrate the robustness of the control to chattering.

Figures 11 and 12 illustrate how the hybrid memory state function α robustly mitigates the noise feedback of the dual quaternions in the

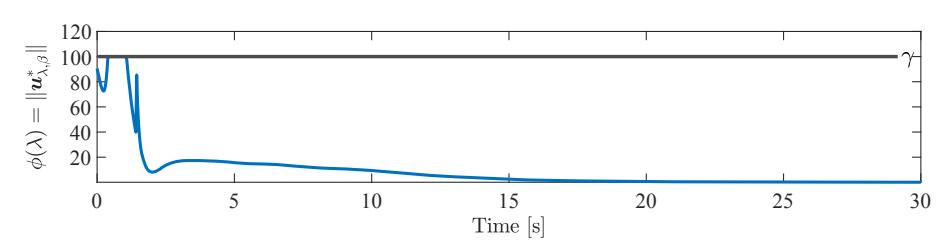


a) Generalized control forces and torques applied to spacecraft base

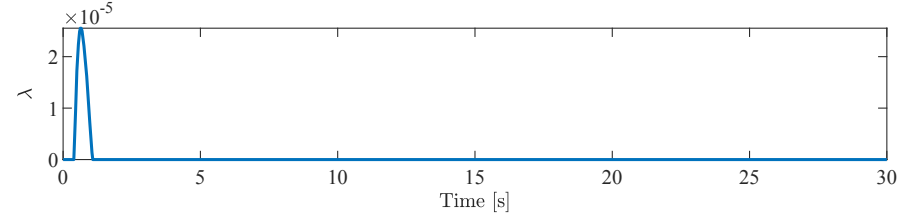


b) Control torques applied to the manipulator

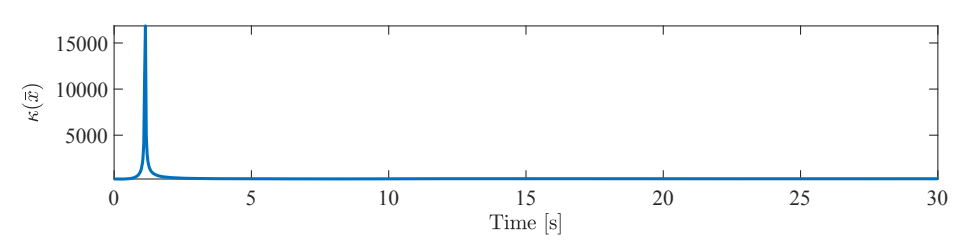
Fig. 13 Reduced real-value dual wrenches applied to the RRRS SMRS during pose stabilization.



a) Norm of control input with damped least-squares permissible value γ



b) Optimal control dampening factor λ



c) Condition number $\kappa(\bar{x})$, of the dynamics matrix $\bar{\Psi}_{1,N}(\bar{x})$

Fig. 14 Optimal damped least-squares actuator allocation during RRRS SMRS pose stabilization.

case of the spacecraft base, and in particular, as shown in Fig. 11a, escapes from $q_{\mathcal{B}_1/\mathcal{S}}^0=0$ without noise-induced chattering.

We also see that the dual control wrenches tend to zero, chatterfree, toward the end of the stabilization maneuver, as shown in Fig. 13.

Finally, we note that selective optimal damped least-square allocation in Eq. (61) did require some dampening of the solution near a singular region near the beginning of the maneuver, but it was only required during transients, as shown in Fig. 14.

VI. Conclusions

A hybrid robust to noise-induced chattering globally asymptotically stable SMRS spacecraft base and end-effector pose-tracking control method has been proposed in this paper. By employing the use of dual quaternions to describe the kinematics and dynamics of SMRSs, we used Lyapunov analysis to derive a global asymptotically stable feedback control law, which allows for coordinated closedloop pose-tracking control of the system. When in the neighborhood of SMRSs' singularities, a damped least-squares allocation policy computes the numerically filtered optimal damping control factor such that it will ensure the feasibility of the solution, i.e., bounded control, with the minimum tracking-solution deviation from the specified trajectory. The effectiveness of the proposed method was illustrated through numerical simulations, showing the controller's capability to 1) simultaneously achieve pose tracking of the spacecraft base and end effector of SMRSs, 2) mitigate singular configurations during transients, 3) alleviate the unwinding phenomena via both positive and negative pole regularization, and 4) provide robustness to chattering from feedback subject to process noise.

The optimal damped least-squares control allocation policy given in Sec. IV is but one allocation technique for *passively* mitigating singularities. We chose to implement this allocation policy because the algorithm is readily deployable for nonredundant multibody systems, at the cost of admitting tracking error in the neighborhoods of singular configurations. Additionally, such damped least-squares allocation effectively can only guarantee that the norm of the collective control input does not exceed a threshold and also does not consider self-colliding configurations into the minimization given in Eq. (55). Hence, our future work will investigate alternative allocation techniques that can *actively* avoid singular configurations inherent in multibody systems, guarantee individual control inputs respect their respective limits, and simultaneously prevent self-colliding configurations without admitting error during pose tracking.

Acknowledgments

This work was supported by a contract from the Aerospace Corporation and from the National Science Foundation through award 2101250. The authors would like to acknowledge the many helpful discussions had with Alfredo Valverde and Mehregan Dor during the preparation of this paper.

References

- [1] Jonsson, A., Morris, R. A., and Pedersen, L., "Autonomy in Space: Current Capabilities and Future Challenge," *AI Magazine*, Vol. 28, No. 4, 2007, p. 27. https://doi.org/10.1609/aimag.v28i4.2066
- [2] Flores-Abad, A., Ma, O., Pham, K., and Ulrich, S., "A Review of Space Robotics Technologies for On-Orbit Servicing," *Progress in Aerospace Sciences*, Vol. 68, 2015, pp. 1–26. https://doi.org/10.2514/6.2015-4426
- [3] Gefke, G., Janas, A., Chiei, R., Sammons, M., and Reed, B. B., "Advances in Robotic Servicing Technology Development," SPACE Conference and Exposition, AIAA Paper 2015-4426, 2015.
- [4] Hu, Q., Dong, H., Zhang, Y., and Ma, G., "Tracking Control of Spacecraft Formation Flying with Collision Avoidance," *Aerospace Science* and Technology, Vol. 42, April 2015, pp. 353–364. https://doi.org/10.1016/j.ast.2014.12.031
- [5] Zhang, D., Song, S., and Pei, R., "Safe Guidance for Autonomous Rendezvous and Docking with a Non-Cooperative Target," *Guidance*, *Navigation*, and Control Conference, AIAA Paper 2010-7592,

- Aug. 2010. https://doi.org/10.2514/6.2010-7592
- [6] Dubowsky, S., and Papadopoulos, E., "The Kinematics, Dynamics, and Control of Free-Flying and Free-Floating Space Robotic Systems," *Transactions on Robotics and Automation*, Vol. 9, No. 5, 1993, pp. 531–543. https://doi.org/10.1109/70.258046
- [7] Yoshida, K., Kurazume, R., and Umetani, Y., "Dual Arm Coordination in Space Free-Flying Robot," *International Conference on Robotics and Automation*, Inst. of Electrical and Electronics Engineers, New York, 1991, pp. 2516–2521. https://doi.org/10.1109/ROBOT.1991.132004
- [8] Papadopoulos, E., and Dubowsky, S., "Dynamic Singularities in Free-Floating Space Manipulators," *Journal of Dynamic Systems, Measure-ment, and Control*, Vol. 115, No. 1, 1993, pp. 44–52. https://doi.org/10.1115/1.2897406
- [9] Yoshida, K., and Umetani, Y., "Control of Space Manipulators with Generalized Jacobian Matrix," *Space Robotics: Dyanmics and Control*, The Kluwer International Series in Engineering and Computer Science, Vol. 188, Springer, Berlin, 1993, pp. 165–204. https://doi.org/10.1007/978-1-4615-3588-1
- [10] Nanos, K., and Papadopoulos, E., "Avoiding Dynamic Singularities in Cartesian Motions of Free-Floating Manipulators," *Transactions on Aerospace and Electronic Systems*, Vol. 51, No. 3, 2015, pp. 2305–2318. https://doi.org/10.1109/TAES.2015.140343
- [11] Carignan, C. R., and Akin, D. L., "The Reaction Stabilization of On-Orbit Robots," *Control Systems Magazine*, Vol. 20, No. 6, 2000, pp. 19–33. https://doi.org/10.1109/37.887446
- [12] Jayakody, H. S., Shi, L., Katupitiya, J., and Kinkaid, N., "Robust Adaptive Coordination Controller for a Spacecraft Equipped with a Robotic Manipulator," *Journal of Guidance, Control, and Dynamics*, Vol. 39, No. 12, 2016, pp. 2699–2711. https://doi.org/10.2514/1.G002145
- [13] Misra, G., and Bai, X., "Optimal Path Planning for Free-Flying Space Manipulators via Sequential Convex Programming," *Journal of Guid-ance, Control, and Dynamics*, Vol. 40, No. 11, 2017, pp. 3019–3026. https://doi.org/10.2514/1.G002487
- [14] Christidi-Loumpasefski, O.-O., Nanos, K., and Papadopoulos, E., "On Parameter Estimation of Flexible Space Manipulator Systems," *International Conference on Intelligent Robots and Systems*, Inst. of Electrical and Electronic Engineers, New York, 2021, pp. 1843–1848. https://doi.org/10.1109/IROS45743.2020.9340768
- [15] Papadopoulos, E., Aghili, F., Ma, O., and Lampariello, R., "Robotic Manipulation and Capture in Space: A Survey," *Frontiers in Robotics and AI*, Vol. 8, July 2021, p. 228. https://doi.org/10.3389/frobt.2021.686723
- [16] Sabatini, M., Gasbarri, P., and Palmerini, G. B., "Coordinated Control of a Space Manipulator Tested by Means of an Air Bearing Free Floating Platform," *Acta Astronautica*, Vol. 139, Oct. 2017, pp. 296–305. https://doi.org/10.1016/j.actaastro.2017.07.015
- [17] Stefano, M. D., Balachandran, R., and Secchi, C., "A Passivity-Based Approach for Simulating Satellite Dynamics with Robots: Discrete-Time Integration and Time-Delay Compensation," *Transactions on Robotics*, Vol. 36, No. 1, 2020, pp. 189–203. https://doi.org/10.1109/TRO.2019.2945883
- [18] Mishra, H., Stefano, M. D., Giordano, A. M., Lampariello, R., and Ott, C., "A Geometric Controller for Fully-Actuated Robotic Capture of a Tumbling Target," *American Control Conference*, Inst. of Electrical and Electronics Engineers, New York, July 2020, pp. 2150–2157. https://doi.org/10.23919/acc45564.2020.9147294
- [19] Filipe, N., and Tsiotras, P., "Rigid Body Motion Tracking Without Linear and Angular Velocity Feedback Using Dual Quaternions," *European Control Conference*, Inst. of Electrical and Electronics Engineers, New York, July 2013, pp. 329–334. https://doi.org/10.23919/ECC.2013.6669564
- [20] Filipe, N., "Nonlinear Pose Control and Estimation for Space Proximity Operations: An Approach Based on Dual Quaternions," Ph.D. Dissertation, Georgia Inst. of Technology, Atlanta, Nov. 2014, http://hdl. handle.net/1853/53055.
- [21] Filipe, N., and Tsiotras, P., "Adaptive Model-Independent Tracking of Rigid Body Position and Attitude Motion with Mass and Inertia Matrix Identification Using Dual Quaternions," *Guidance, Navigation, and Control Conference*, AIAA Paper 2013-5173, Boston, MA, Aug. 2013. https://doi.org/10.2514/6.2013-5173
- [22] Filipe, N., and Tsiotras, P., "Simultaneous Position and Attitude Control Without Linear and Angular Velocity Feedback Using Dual Quaternions," American Control Conference, Inst. of Electrical and Electronics

- Engineers, New York, June 2013, pp. 4808–4813. https://doi.org/10.1109/ACC.2013.6580582
- [23] Valverde, A., and Tsiotras, P., "Spacecraft Robot Kinematics Using Dual Quaternions," *Robotics*, Vol. 7, No. 4, 2018, p. 64. https://doi.org/10.3390/robotics7040064
- [24] Valverde, A., and Tsiotras, P., "Dual Quaternion Framework for Modeling of Spacecraft-Mounted Multibody Robotic Systems," Frontiers in Robotics and AI, Vol. 5, Nov. 2018, p. 128. https://doi.org/10.3389/frobt.2018.00128
- [25] Valverde, A., "Dynamic Modeling and Control of Spacecraft Robotic Systems Using Dual Quaternions," Ph.D. Dissertation, Georgia Inst. of Technology, Atlanta, GA, April 2018, http://hdl.handle.net/1853/ 59928
- [26] Tsiotras, P., King-Smith, M., and Ticozzi, L., "Spacecraft-Mounted Robotics," *Annual Review of Control, Robotics, and Autonomous Systems*, Vol. 6, No. 1, 2023, pp. 335–362. https://doi.org/10.1146/annurev-control-062122-082114
- [27] Mayhew, C. G., Sanfelice, R. G., and Teel, A. R., "Robust Global Asymptotic Attitude Stabilization of a Rigid Body by Quaternion-Based Hybrid Feedback," *Conference on Decision and Control Held Jointly with Chinese Control Conference*, Inst. of Electrical and Electronics Engineers, New York, Dec. 2009, pp. 2522–2527. https://doi.org/10.1109/cdc.2009.5400431
- [28] Mayhew, C. G., Sanfelice, R. G., and Teel, A. R., "Quaternion-Based Hybrid Control for Robust Global Attitude Tracking," *Transactions on Automatic Control*, Vol. 56, No. 11, 2011, pp. 2555–2566. https://doi.org/10.1109/TAC.2011.2108490
- [29] Bhat, S. P., and Bernstein, D. S., "A Topological Obstruction to Continuous Global Stabilization of Rotational Motion and the Unwinding Phenomenon," *Systems & Control Letters*, Vol. 39, No. 1, 2000, pp. 63–70. https://doi.org/10.1016/S0167-6911(99)00090-0
- [30] Mayhew, C. G., Sanfelice, R. G., and Teel, A. R., "On Path-Lifting Mechanisms and Unwinding in Quaternion-Based Attitude Control," *Transactions on Automatic Control*, Vol. 58, No. 5, 2013, pp. 1179– 1191. https://doi.org/10.1109/TAC.2012.2235731
- [31] Yang, J., and Stoll, E., "Adaptive Sliding Mode Control for Spacecraft Proximity Operations Based on Dual Quaternions," *Journal of Guidance, Control, and Dynamics*, Vol. 42, No. 11, 2019, pp. 2356–2368. https://doi.org/10.2514/1.G004435
- [32] Malladi, B. P., Butcher, E. A., and Sanfelice, R. G., "Rigid-Body Pose Hybrid Control Using Dual Quaternions: Global Asymptotic Stabilization and Robustness," *Journal of Guidance, Control, and Dynamics*,

- Vol. 43, No. 9, 2020, pp. 1631–1641. https://doi.org/10.2514/1.G004621
- [33] Brodsky, V., and Shoham, M., "Dual Numbers Representation of Rigid Body Dynamics," *Mechanism and Machine Theory*, Vol. 34, No. 5, 1999, pp. 693–718. https://doi.org/10.1016/S0094-114X(98)00049-4
- [34] Wang, J., and Sun, Z., "6-DOF Robust Adaptive Terminal Sliding Mode Control for Spacecraft Formation Flying," *Acta Astronautica*, Vol. 73, April 2012, pp. 76–87. https://doi.org/10.1016/j.actaastro.2011.12.005
- [35] Haddad, W. M., and Chellaboina, V., Nonlinear Dynamical Systems and Control: A Lyapunov-Based Approach, Princeton Univ. Press, Princeton, NJ, 2011, pp. 3–4.
- [36] Deo, A. S., and Walker, I. D., "Optimal Damped Least-Squares Methods for Inverse Kinematics of Robot Manipulators," *Cooperative Intelligent Robotics in Space II Proceedings*, edited by W. E. Stoney, Soc. of Photo-Optical Instrumentation Engineers, Bellingham, Washington, D.C., Nov. 1992, pp. 123–138. https://doi.org/10.1117/12.56752
- [37] Deo, A. S., and Walker, I. D., "Overview of Damped Least-Squares Methods for Inverse Kinematics of Robot Manipulators," *Journal of Intelligent & Robotic Systems*, Vol. 14, No. 1, 1995, pp. 43–68. https://doi.org/10.1007/BF01254007
- [38] Jung, D., and Tsiotras, P., "An Experimental Comparison of CMG Steering Control Laws," Astrodynamics Specialist Conference and Exhibit, AIAA Paper 2004-7592, Aug. 2004. https://doi.org/10.2514/6.2004-5294
- [39] Maciejewski, A. A., and Klein, C. A., "Numerical Filtering for the Operation of Robotic Manipulators Through Kinematically Singular Configurations," *Journal of Robotic Systems*, Vol. 5, No. 6, 1988, pp. 527–552. https://doi.org/10.1002/rob.4620050603
- [40] Chiaverini, S., "Estimate of the Two Smallest Singular Values of the Jacobian Matrix: Application to Damped Least-Squares Inverse Kinematics," *Journal of Robotic Systems*, Vol. 10, No. 8, 1993, pp. 991– 1008. https://doi.org/10.1002/rob.4620100802
- [41] Chiaverini, S., Egeland, O., and Kanestrom, R., "Achieving User-Defined Accuracy with Damped Least-Squares Inverse Kinematics," Fifth International Conference on Advanced Robotics, Inst. of Electrical and Electronics Engineers, New York, June 1991, pp. 672–677. https://doi.org/10.1109/icar.1991.240676
- [42] NASA-3D-Resources, NASA, Oct. 2015, https://github.com/nasa/ NASA-3D-Resources.